MOLECULARLY-COMPLETE PLANAR SUPPORTED CELL PLASMA MEMBRANES AS SCAFFOLDS FOR BIOMEDICAL APPLICATIONS

A Thesis

Presented to the Faculty of the Graduate School

of Cornell University

In Partial Fulfillment of the Requirements for the Degree of

Master of Science

by

Han-Yuan Liu

[August 2017]

ABSTRACT

Emerging technologies to study membrane proteins, protein-lipid interactions, and to create new kinds of sensing and analytical devices, use cell plasma membrane vesicles or ‘blebs’ as an intermediate to form molecularly complete, planar cell surface mimetics that are compatible with a variety of characterization tools and microscopy methods. This approach enables direct incorporation of membrane proteins into supported lipid bilayers without using detergents and reconstitution, preserving the native lipids and other species within the plasma membrane. However, the impact of methods used to induce cell blebbing (vesiculation) on protein and membrane properties is still unknown. This study focuses on characterization of the cell blebs created under various bleb-inducing conditions and its result on protein behavior (orientation, mobility, activity, *etc*.) and lipid scrambling in this platform. (Chapter 1) This work enriches our understanding of cell plasma membrane bleb bilayers as a biomimetic platform and represents one of few ways to make molecularly-complete supported bilayers from cell membranes. Such a model system can be widely applied to studies aimed at understanding the roles of membrane proteins as drug targets in drug delivery, in virus-host interactions, and in tissue engineering platforms, among many other bioanalytical and sensing applications. Here, we applied this biomimetic model system to studies of oncogenic micrcrovesicle interaction with stem cell surface. Combined with TIRF, the impact of microenvironment on binding and entry of microvesicle to stem cell surface will be revealed at the single particle level. (Chapter 2)

BIOGRAPHICAL SKETCH

Han-Yuan Liu was born in Taipei, Taiwan to Su-Hua Yang and Wen-Bin Liu on January 1st 1991. He joined Chemical Engineering from National Taiwan University in August 2010. After receiving his B.S degree in June 2014, He further went on to pursue a M.S degree at Department of Chemical and Biomolecular Engineering at Cornell University in Prof. Susan Daniel's group in August 2015.

I dedicate this thesis to my family, friends and all members of the Cornell community that supported me over my graduate study.

ACKNOWLEDGMENTS

The research presented in this thesis would not have been possible without the generous help and support of members of the Cornell community. First and foremost I would like to thank my advisor, Prof. Susan Daniel and my special committee members, Prof. Matthew J. Paszek and Prof. Claudia Fischbach-Teschl. I thank all the members of the Daniel Research Group. I would also like to thank the Fischbach Research Group for support and help in learning about oncogenic microvesicles. I would like to thank Prof. Gijs Wuite and Wuite research group in Vrije Universiteit Amsterdam for help in characterizing bleb morphology and mechanical resilience. I would like to thank Prof. Christopher K. Ober and Ober research group for support and help in learning polyelectrolyte brushes. Finally, I would like to thank my parents and my sister. All of this would not be possible without them. Grants and funding are acknowledged at the end of each chapter.

TABLE OF CONTENTS

LIST OF FIGURES

LIST OF ABBREVIATIONS

ASCs – human adipose-derived stem cells

BHK – baby hamster kidney

DTT – dithiothreitol

FA – formaldehyde

FRAP – fluorescence recovery after photobleaching

GPI-YFP – glycophosphatidylinositol anchored yellow fluorescent protein

hAPN – human alanine aminopeptidase

MDAs – MDA MB-231 human metastatic breast cancer cells

MSD – mean squared displacement

MSS – moment scaling spectrum

PDMS – polydimethylsiloxane

R18 – Octadecyl Rhodamine B chloride

SS – serum starving

SPT – single particle tracking

TIRFM – total internal reflection fluorescence microscopy

CHAPTER 1

PLANAR MAMMALIAN MEMBRANE AS MODELS OF IN VIVO CELL SURFACE ARCHITECTURES

1.1. Introduction

Biological membranes comprised of phospholipids and proteins are a specialized permeability barrier encapsulating the cell cytosol and organelles and are important for regulating the interaction between cells and their external environment. Proteins in biological membranes have critical roles in molecular-scale processes necessary to cell function, such as material transport, signaling, and recognition.[1, 2, 3, 4] Furthermore, interactions of lipids with proteins are crucial for regulating protein activity in these various roles.[5, 6] In order to understand how lipid-protein interactions regulate membrane protein function in biological membranes, cell-based assays are conventionally used. The advantage of cell-based assay is the ability to preserve the native environment. However, the complexity and dynamism of cells makes such assays inconvenient for isolating the effect of individual factors on the studies at hand. On the other hand, the traditional characterization techniques for lipid-protein interaction using detergents to extract membrane proteins change the structure and function of proteins and may artificially change the native lipid-protein association.[5, 7, 8] Thus, alternative membrane platforms that bridge *in vivo* and *in vitro* environments and are compatible with a wide variety of characterization techniques can greatly assist in understanding how membrane proteins function and are regulated. Such platforms can also be employed in a variety of bioanalytical and sensing applications,

which leverage the relationship between protein and lipid on biological function.

A supported lipid bilayer (SLB) can be formed on a solid surface using vesicle rupture or Langmuir-Blodgett-Schaeffer transfer techniques. Because of its planar geometry, the SLB is compatible with various surface characterization tools such as total internal reflection microscopy (TIRFM)[9], atomic force microscopy (AFM)[10], quartz crystal microbalance (QCM)[11], and surface plasmon resonance (SPR)[12]. However, the challenges of incorporating membrane proteins into SLBs are significant, namely with regard to their orientation, fluidity, and function. In our previous work[13, 14, 15], we demonstrated that membrane proteins can be introduced into SLBs using the cell plasma membrane 'blebs' without using detergents or vesicle reconstitution **(Fig. 1A)**. Cell plasma membrane blebs are proteoliposomes that bud from the cell surface, induced by either chemical reagents or serum starving. These proteoliposomes retain the lipid and protein diversity of the cellular membrane. Although cell blebbing allows the incorporation of membrane protein into SLBs without the need for detergents and reconstitution, there are key aspects that need to be investigated regarding the impact of the means by which blebs are produced (chemical versus chemical-free), on protein and lipid properties, namely protein orientation, mobility, level, activity, and membrane leaflet asymmetry.

Formaldehyde (FA) and dithiothreitol (DTT) are commonly used in chemical blebbing process. FA is known to be a protein cross-linking agent when applied to cells at higher concentrations (4%).[16, 17] DTT reduces disulfide bonds and palmitoylated cysteines, which can impact lipid phase partitioning.[17, 18, 19] To investigate the impact of chemical and chemical-free means on producing cell

membrane blebs and cell membrane bleb bilayers, we varied the concentration of FA/DTT in blebbing solutions, or employed serum starving to induce baby hamster kidney (BHK) to vesiculate, or "bleb". The resulting blebs were characterized for size, charge, and concentration and stiffness. Blebs and planar bilayers formed from them were characterized for protein content and protein and lipid orientation. Protein mobility, confinement, and activity were assessed in planar bilayers.

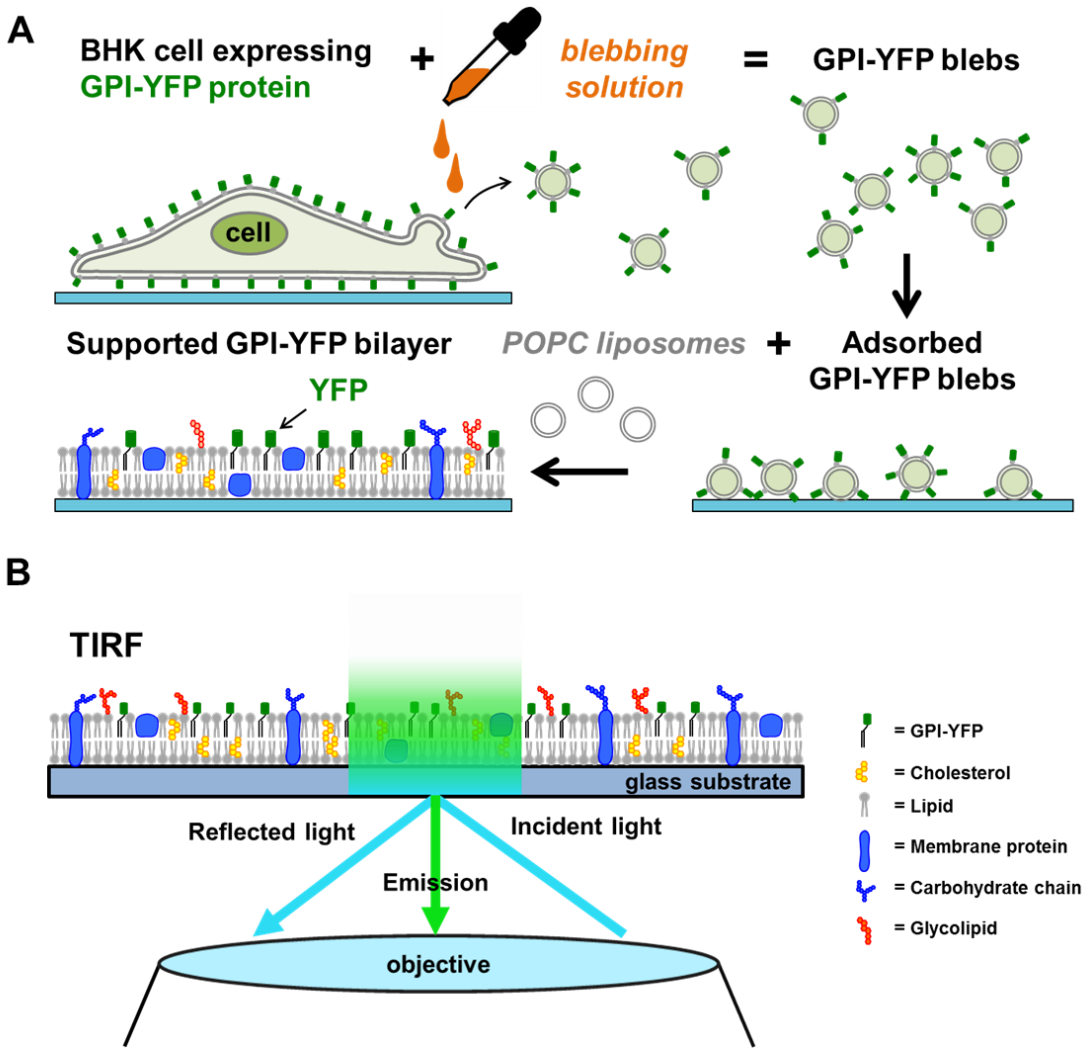

Figure 1. Blebbing and TIRF (A) BHK cells expressing GPI-YFP were induced to generate the cell plasma membrane blebs via blebbing process, and then cell plasma membrane bleb bilayer formed by using the cell blebs as intermediate. (B) TIRF was applied to investigate the protein behavior in cell plasma membrane bleb bilayer.

Glycophosphatidylinositol proteins (with lipid anchor) are located at the extracellular leaflet of the plasma membrane and are involved in variety of biological process such as signaling, catalysis, enzymatic, and cell adhesion.[20, 21] Combined with total internal reflection microscopy (TIRFM), SLBs formed from cell plasma membrane blebs expressing glycophosphatidylinositol anchored yellow fluorescent protein (GPI-YFP) provides a simple way to study protein mobility via single particle tracking (SPT) **(Fig. 1B)**. With SPT, single fluorescent proteins are tracked and analyzed to determine the protein mobility, diffusivity and confinement trends under various blebbing conditions. To assess protein orientation, a protease cleavage assay was used to indicate the orientation of GPI-YFP. To assess lipid asymmetry, PS lipid orientation in cell plasma membrane blebs and cell plasma membrane bleb bilayer was revealed through an annexin V binding assay. To assess protein activity under various blebbing conditions, human aminopeptidase N (hAPN), a membrane-bound enzyme, was subjected to an enzyme activity assay. hAPN plays multiple roles in physiological processes including metabolism, cell motility and adhesion, and coronavirus binding and entry.[22, 23, 24] hAPN expression levels under these different blebbing conditions was revealed via immunoblotting.

In this work, we find that cell membrane bleb bilayers as a biomimetic mammalian platform preserve the protein orientation, mobility, and activity. One drawback we discovered is that PS lipid asymmetry is not maintained. Nonetheless, this platform is still a powerful tool for *in vitro* applications, having identified conditions where protein properties are best maintained. By combining planar cell

membrane bleb bilayers with appropriate surface characterization techniques, these materials have been shown to be convenient platforms to quantitatively measure virus binding and entry [14, 15]. With the complete characterization presented here, such a molecularly complete planar supported cell membrane with maximally functional proteins could be useful for myriad technological purposes from tissue engineering, to drug delivery screening, to advanced studies of virus binding and entry.

1.2. Materials and methods

1.2.1. Cells and plasmids

Baby hamster kidney (BHK) cells are extensively used as successful host for stable expression of various recombinant proteins, substrate for virus propagation for vaccine, and crucial member of mammalian expression systems for pharmaceutical production.[25, 26, 27] BHK cells used in our work were obtained from the American Type Culture Collection (ATCC) and grown in Dulbecco's modified Eagle medium (DMEM) (CellGro) supplemented with 10% fetal bovine serum (Gibco), 100 U/ml penicillin and 10 μg/ml streptomycin (CellGro), 1% HEPES buffer (CellGro). The pYFP-GPI-N1 plasmid was obtained from the Baird/Howlawka research group at Cornell University and used for transfection of BHK cells to express a glycophosphatidylinositol (GPI) anchored yellow fluorescent (YFP) protein. The pCI-neo-hAPN plasmid was the generous gift from Kathryn Holmes of the University of Colorado and used for transfection of BHK cells to express the human aminopeptidase N (hAPN).

1.2.2. Preparation of liposomes

The following lipids were used in these experiments. 1-oleoyl-2-palmitoyl-sn-glycero-3-phosphocholine (POPC) and 1-palmitoyl-2-oleoyl-*sn*-glycero-3-phospho-L-serine (POPS), purchased from Avanti Polar Lipids. The liposomes were prepared by mixing the components in the chloroform (Sigma) in the desired ratio. Chloroform was gently evaporated using a stream of nitrogen, then the lipid films were stored under vacuum for 3 hours to remove any residual chloroform. To create liposomes, phosphate buffered saline (PBS) buffer (5mM NaH_2PO_4, 5mM Na_2HPO_4, 150mM NaCl at pH 7.4) was added to the dried films to the concentration of 2 mg/ml. Single unilamellar liposomes were prepared by extrusion using a 50 nm membrane with at least 15 passes. Two formulations were used in this study: The first is pure POPC and the second contains 98% POPC and 2% POPS. The first preparation, POPC liposomes, is used in forming the supported lipid bilayer with the cell plasma membrane blebs. The second formulation, POPC 98% POPS 2% liposomes, is used to form the supported lipid bilayer containing PS to verify the binding of Annexin V-FITC (Molecular Probes) as a control.

1.2.3. Preparation of plasma cell membrane blebs

6 ml of 1.5×10^6 cells/ml cells were seeded in 10 cm Petri dishes (Corning) and incubated for 24 hours in a 37 °C, 5% CO_2 incubator. Transfection was performed by using 18 μL of Turbofect transfection reagent (ThermoScientific) and 6 μg of DNA plasmid, pYFP-GPI-N1, and incubated for 24 hours in a 37 °C, 5% CO_2 incubator. After 24 hours, the cells were washed with GPMV buffer (2 mM $CaCl_2$, 10 mM HEPES, 150 mM NaCl at pH 7.4), and 4 ml of GPMV buffer with 25 mM formaldehyde (FA) and 2 mM dithiothreitol (DTT) (0.075%FA) was used to induce

the cell blebs subsequently. Various concentrations of blebbing solution (0.01 %FA, 0.075 %FA, 1.5 %FA, 3.0 %FA, 4.0 %FA) were used in these studies. The cells were incubated in the blebbing solution for 1 hour at 37 °C. The other method used here to perform the cell blebbing is serum starving (SS) of the BHK cells. Here cells were washed by 6 ml Dulbecco's modified Eagle medium, and 4 ml of Dulbecco's modified Eagle medium without fetal bovine serum. This mixture was added into the plates to induce the cell blebbing. In both cases, after incubation for 1 hour at 37 °C, cell blebs were settled on ice for 15 min to separate cell debris and cell blebs were collected from the supernatant.

1.2.4 AFM characterization of bleb resilience and morphology

Blebs were attached to poly-L-lysine coated glass slides in their corresponding buffer. Slides were first cleaned in a 96% ethanol, 3% HCl solution for 10 minutes. Next they were coated for 1 hour in a 0.001% poly-L-lysine (Sigma) solution, rinsed with ultrapure water, and dried overnight at 37 ^{0}C. Coated slides were stored at 7 ^{0}C for maximum 1 month. Blebs were imaged in PeakForce Tapping^{TM} mode on a Bruker Bioscope catalyst setup. Force set point during imaging was 100 pN - 200 pN. Nano-indentations were performed by first making an image of a single particle, then indenting it until a trigger force of 0.5 nN is reached, and subsequently higher forces of 10-20 nN at a velocity of 250 nms^{-1}. After indentation, typically another image was recorded to check for movement or collapse of the vesicle. Importantly, both before and after the vesicle indentation, the tip was checked for adherent lipid bilayers by obtaining a force curve on a glass surface until a force of 5 nN. Tips used were either silicon nitride tips with a nominal tip radius of 15 nm on a 0.1 N/m cantilever by

Olympus (OMCL-RC800PSA) or Bruker SNL silicon nitride tips on a 0.12 N/m cantilever with a nominal tip radius of 2 nm. All the presented force spectroscopy data was obtained using Bruker SNL cantilevers. Individual cantilevers were calibrated using thermal tuning. Data analysis of nano-indentation curves was done using Gwydion software.

1.2.5. Characterization of bleb size, charge, and concentration

Nanosight NS300 (Malvern) was used to determine the size and concentration of blebs in the supernatant. Zetasizer Nano ZS (Malvern) was used to measure the charge of blebs with Laser Doppler Micro-electrophoresis. For measurement of charge, serum-starved blebs were measured in Dulbecco's modified Eagle medium and chemical-induced blebs were measured in GPMV buffer.

1.2.6. Preparation for bleb planar bilayer formation

Polydimethylsiloxane (PDMS) wells were made by 10:1 elastomer/crosslinker mixture of Sylgard 184 (Robert McKeown Company) and baked for 5 hours at 78°C. PDMS wells were attached to the dry clean glass slides (25×25 mm No.1.5, VWR). The glass slides were pretreated by piranha solution (70% (v/v) H_2SO_4 (BDH) and 30% (v/v) H_2O_2 (Sigma 50 wt %)) for 10 min and rinsed by flushing DI water 20 min continuously. Then 100 μL of solution containing blebs at approximately 5×10^8 blebs/mL was added into the well and incubated for 15 min. After incubation, the well was rinsed gently with PBS buffer to remove the unattached blebs. The 100 μL liposomes at 2 mg/mL was added into the well continuously and incubated for 30 min to form the bleb bilayer. After the bleb bilayer formed, the well was rinsed with PBS buffer again to remove the excess liposomes.

1.2.7. Protease cleavage assay for protein orientation in cell blebs and planar bleb bilayers

Proteinase K (Sigma) in the form of lyophilized powder was added to the storage buffer (20 mM Tris-HCl, 1 mM $CaCl_2$, 50% glycerol at pH 7.4) at 20 mg/mL and stored at -20°C. Proteinase K was diluted to 100μg/mL by used buffer (20 mM Tris-HCl at pH 7.4) to conduct the protease cleavage assay. For determination of GPI-YFP orientation in the either blebs or bleb bilayer, 100 μL of 100 μg/mL proteinase K was added to either blebs or bleb bilayer on glass slides from various blebbing conditions. Images were recorded at 15 min interval to track proteinase K cleavage registered when the fluorescent domain of protein leaves the evanescent field resulting in the loss of fluorescent signals in blebs and bleb bilayer. This loss was quantified by particle counting. The number of fluorescent particles was compared to the control samples without adding the proteinase K. The results reveal the orientation of GPI-YFP in the blebs and bleb bilayer.

1.2.8. Annexin V assay for lipid orientation in cell blebs and planar bleb bilayers

Annexin V conjugated with FITC is a protein that preferentially binds phosphatidylserine (PS) and is strongly calcium-dependent. PS is commonly found on the internal leaflet of cell plasma membrane of live cells. At the early process of apoptosis, the symmetry of phospholipid is disrupted such that PS becomes exposed on the external leaflet of cell plasma membrane.[28] BHK cells expressing hAPN were rinsed with binding buffer (10 mM Tris, 100 mM NaCl, and 8 mM $CaCl_2$ at pH 7.4) and added 5 μL annexin V incubated for 30 min. After incubation, the cells were rinsed with PBS buffer. In serum starving and 0.075 %FA cases, the cells were treated

by same procedure mentioned above of annexin V binding after blebbing process. The images of BHK cells were recorded by inverted Zeiss Axio Observer.Z1 microscope with α Plan-Apochromat 20× objective. 100 μL POPC liposomes and POPC 98%, POPS 2% liposomes at 2 mg/mL were added respectively to the wells and incubated for 30 min. After incubation, the wells were rinsed with binding buffer and added 2 μL annexin V incubated for 30 min. Then the wells were rinsed with PBS buffer to remove the excess unbound annexin V. The blebs on glass slides were rinsed with bovine serum albumin (BSA, Sigma) at 0.1 mg/mL for 30 min. The bleb bilayers on glass slides were rinsed with BSA at 0.01 mg/mL for 30 min. Both wells were rinsed with binding buffer and added 2 μL annexin V incubated for 30 min. Then the wells were rinsed with PBS buffer to remove the excess unbound annexin V.

1.2.9. Characterization of motion of individual membrane proteins by single particle tracking

Bleb bilayers incorporating the fluorescent protein, GPI-YFP, were imaged and recorded by total internal reflection microscopy (TIRF). The settings and operation of microscope are described below.

Various methods for single particle tracking (SPT) have already been described in previous literature.[29, 30, 31, 32]. To enable accurate tracking, all the trajectories were found and calculated by using the single particle tracking method previously reported by Richards et al.[13]. This method determined the particle location by their intensity, change of intensity from previous frame, and displacement from previous frame to find the match for every trajectory.[33] A particle that only moves around inside an area smaller than the maximum observed displacement for immobile

fluorescent beads in the system is regarded as immobile.[34] The single particle tracking algorithm uses the initial slope of the mean squared displacement (MSD) from the first three time steps to determine the local "homogenous" diffusion coefficient.[35, 36] Therefore, the heterogeneity of bleb bilayer or change of diffusion mode resulting from different domains does not strongly influence the initial diffusion coefficient for short times. To assess this heterogeneity, we employ moment scaling spectrum (MSS) analysis reported by Ferrari et al.[32, 34] to quantify the mobility of a particle via parameter β. Here, the parameter β describes the type of motion for each particle. $B < 0.4$ is confined diffusion. $0.4 \leq \beta \leq 0.6$ is quasi-free diffusion. $\beta > 0.6$ is convective diffusion. All the images were analyzed by using Matlab (Mathworks) and ImageJ (NIH).

1.2.10. Human aminopeptidase N enzyme (hAPN) activity assay

Human aminopeptidase N is widely expressed in many cell types and species plays crucial roles in many biological processes such as cell adhesion, peptide metabolism, and coronaviruses binding. Human aminopeptidase N, membrane-bound enzyme, also cleaves the N-terminal amino acid from active protein leading to the inactivation.[22, 23, 24] To analyze the impact of formaldehyde on the native enzymatic function of hAPN, the enzymatic activity assay was conducted to reveal the activity of hAPN in blebs from various blebbing conditions. The activity of hAPN in blebs was measured with a fluorometer (Photon Technologies International Inc.) at an excitation/emission of 380/460 nm. H-Ala-AMC (Bachem) is the substrate for hAPN. As the hAPN cleaves the substrate, the substrate becomes fluorescent. Bleb concentration was controlled at 5×10^8 blebs/mL during these experiments. Mixture of

500 μL blebs and 500 μL H-Ala-AMC at 270 mM in a 50 mM Tris buffer at pH 7.4 were added to a cuvette and the fluorescent intensity was monitored for 1.5 hour.

1.2.11. Characterization of protein expression by Western blot

After the blebbing process induced by either serum starving or FA/DTT exposure, cell blebs were concentrated by ultracentrifuge in preparation for Western blotting. First, the bleb concentration was measured and adjusted to be the same across all samples using a Nanosight instrument. Next, these samples of cell blebs were centrifuged at 30,000×g for 1 hr and the pellets were resuspended by GPMV buffer. The samples were mixed with 2× Laemmli sample buffer (Bio-Rad) plus 10% DTT at 1:1 ratio. The samples were incubated at 50°C for 10 min. Then, the samples were separated by SDS-PAGE (Bio-Rad) and transferred to PVDF membrane (Millipore). The membrane was blocked with 5% dry fat milk in Tris-buffered saline plus 0.01% Tween-20 (TBST) at room temperature for 1 hour and the membrane was incubated with 1:1000 anti-hAPN antibodies (Everest Biotech) at room temperature for 1 hour. After washing with TBST, the membrane was rinsed in 1:2500 Horseradish Peroxidase conjugated-rabbit anti-goat IgG antibodies (abcam). In GPI-YFP case, the membrane was incubated with 1:2500 anti-GFP antibodies and then 1:2500 Horseradish Peroxidase conjugated-rabbit anti-mouse IgG antibodies. After washing with TBST, protein bands were visualized by ECL detection system (Bio-Rad).

1.2.12. TIRF microscope settings and operation

The GPI-YFP protein orientation, motion tracking, and annexin V binding for lipid orientation were conducted using total internal reflection fluorescence (TIRF) microscopy on an inverted Zeiss Axio Observer.Z1 microscope with an α Plan-

Apochromat 100× objective. 488 nm and 561 nm wavelength from solid-state lasers were used to excite the sample. A Laser TIRF 3 slider (Carl Zeiss, Inc.) was used to control angle of incidence at ~68° generating the evanescent wave around 100 nm and total internal reflection. The excitation light was filtered by Semrock LF488-B-ZHE filter cube and sent to the electron multiplying CCD camera (ImageEM C9100-13, Hamamatsu).

1.3. Results and discussion

1.3.1. Characterization of bleb size, charge, and concentration

To investigate the impact of the chemicals used to induce blebbing on the properties of cell membrane blebs, six solutions covering a range of concentrations of chemicals were examined. These are denoted as 0.01%, 0.075%, 1.5%, 3% and 4% formaldehyde (FA) with the appropriate amount of DTT to maintain the ratio of FA/DTT in GPMV buffer; DMEM was used for the serum starving (SS) method (0% FA/DTT). The resulting blebs were examined using a Zetasizer or Nanosight instrument to assess their average size, charge, and concentration. We found that the charges of blebs from various blebbing conditions were similar, at about -12 mV, which indicates that increasing FA/DTT concentration in blebbing solutions has minimal effect on the charge of blebs **(Fig. 2A)**. However, the size of blebs slightly increases with the increasing concentration of FA/DTT **(Fig. 2B)**. The size range of cell blebs is between 100 - 500 nm with the average size of cell blebs at 150 - 200 nm. The concentrations of cell blebs isolated in the supernatant were consistently around 10^8-10^9 blebs/ml among all blebbing conditions **(Fig. 2C)**. In summary, the average

size of the cell blebs increases about 50 nm with increasing concentration of FA/DTT used in the blebbing solution. However, increasing FA/DTT does not affect the concentration or the charge of cell blebs over the range tested here, including the serum-starving case.

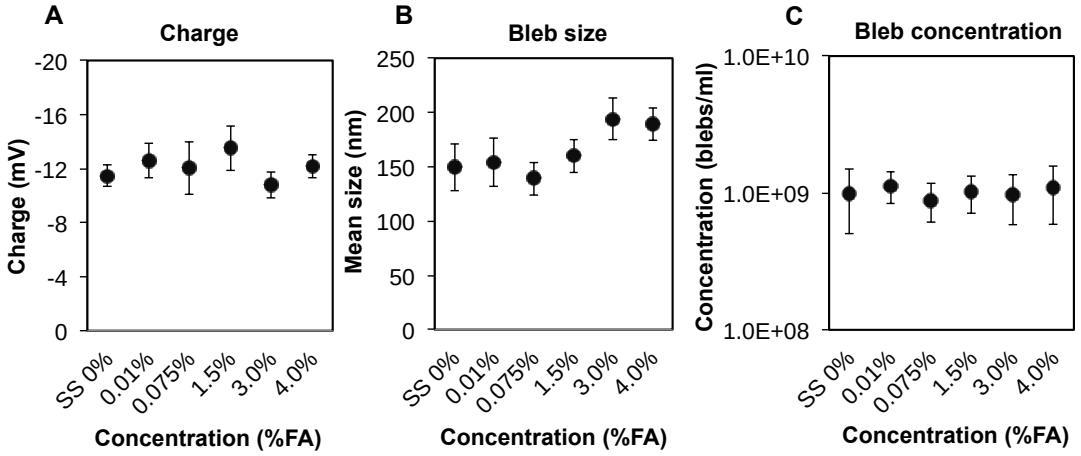

Figure 2. Blebs charge, size, and concentration characterization. (A) The blebs are produced by various FA/DTT conditions and the charges of blebs are about -12 mV. (B) The average size of the cell blebs increases slightly with increasing concentration of FA/DTT in the blebbing solution. (C) The concentrations of cell blebs are similar with the increasing concentration of FA/DTT.

1.3.2 Characterization of bleb morphology and mechanical resilience by AFM

Blebs were further characterized by AFM imaging and force spectroscopy. A typical image of an individual bleb, formed using 0.01% FA, is shown in **Fig. 3A**. Following imaging, force indentation curves were obtained on individual blebs at their highest point. Due to rupturing of vesicles, a relatively small number of force plots were collected. **Figure 3** summarizes the breakthrough force data that we collected. The breakthrough force is defined as the force required for the tip to break through the bilayer, as shown in a typical plot in **Fig. 3B** for 0.01% FA generated blebs, and

depicted in the cartoon inset. In can be seen in **Fig. 3C** that the 4% FA blebs are significantly more resilient than the 0.01% FA or 0.075% blebs, as the mean force required to break 4% FA blebs is about three times higher. Serum-starvation generated blebs are even stiffer, almost four times higher.

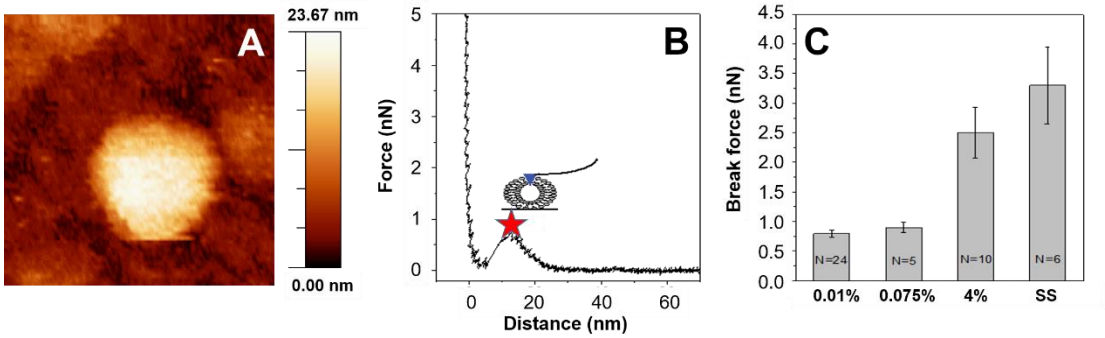

Figure 3. (A) A typical images of an adsorbed bleb (0.01% FA) on a PLL protein surface prior to indentation. (B) A typical force-distance curve obtained on a 0.01% FA bleb. The cartoon inset shows a schematic depiction of the breakthrough event. Asterisk marks location of break event. (C) Breakthrough forces of blebs at four different blebbing conditions, 0.01%, 0.075%, 0.4% FA, and serum-starved (SS). (Figure contributed by: Raya Sorkin and Filip Bošković in Wuite research group at Vrije Universiteit Amsterdam)

These results demonstrate that blebbing conditions have impact on the resilience of blebs, and therefore may directly affect rupture efficiency. Differences in rupture efficiency may, in turn, lead to differences in observed protein mobility, which we examine later. It is therefore important to select the optimal blebbing conditions, which would allow efficient rupture of blebs and sufficient protein mobility.

Despite using low scanning forces of 100 pN, we observed rupture of vesicular structures and local formation of planar bilayers for all bleb samples (**Fig. 4**). Typical cross sections at each blebbing condition are shown in beneath the images, where it can be clearly seen that the thicknesses of the formed layers correspond to typical

planar single bilayer thickness of ~4 nm. We note that small areas of higher thickness are seen in the bilayers, most likely corresponding to proteins embedded in the bilayer. However, larger glycocalyx structures were not detected by AFM in these measurements. It is possible that the cell blebs don't contain these large sugar groups or that they are too dilute or soft to detect in the final bilayer with the AFM tip.

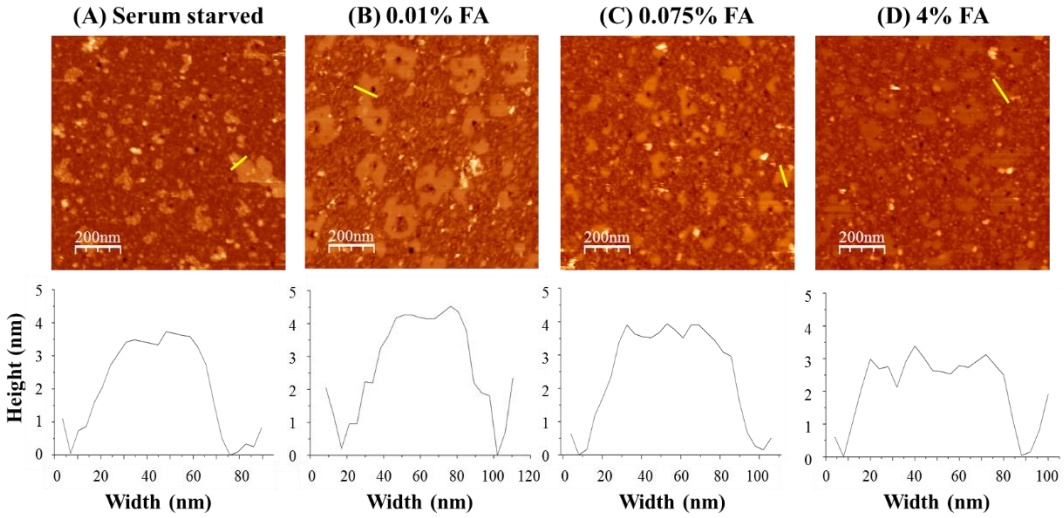

Figure 4. AFM images of ruptured bleb patches on glass surfaces. (A) Serum starved, (B) 0.01.5 FA, (C) 0.075% FA, and (D) 4% FA. Cross-sections below each image show typical bilayer thickness corresponding to the yellow line in the image above, demonstrating that blebs rupture and form a planar structure. (Figure contributed by: Raya Sorkin and Filip Bošković in Wuite research group at Vrije Universiteit Amsterdam)

1.3.3. Cell membrane bleb bilayer formation

Cell plasma membrane blebs generally do not rupture to form the contiguous, planar bilayer by themselves. Therefore, fusogenic lipid vesicles are used to facilitate rupture of cell blebs and healing together of isolated bilayer patches. Harvested cell blebs were added into PDMS well and incubated on the glass substrate directly. After incubation, POPC liposomes were added into PDMS well to commence planar bilayer formation and healing (**Fig. 1**). In previous work[13], the mechanism of formation of

planar bleb bilayer was verified by quartz crystal microbalance (QCM-D) measurements and direct observation of membrane-bound fluorescent species diffusing from ruptured blebs. Although previous work verified the formation of planar bleb bilayers, to use the planar bleb bilayer as biomimetic platform requires protein orientation to be the same as native mammalian cells. In the next sections, we present our results on investigations of the impact of various blebbing conditions on protein and lipid orientation in both cell blebs and bleb bilayers.

1.3.4. Characterization of GPI-YFP protein orientation in blebs and planar bilayers

Important features of mammalian cell blebs are their abilities to be transformed into supported planar bilayers that mimic many features of cell membranes, including their composition and protein content. Hence, understanding the impact of FA/DTT exposure or serum starving on the protein orientation in cell blebs and bleb bilayer is paramount for creating a useful biomimetic material. In order to verify the protein orientation, GPI-YFP plasmid was transfected into the BHK cells and followed by various bleb-inducing treatments. Assessing protein orientation in blebs and bleb bilayers was carried out by a protease assay. GPI-linked protein is a monotopic peripheral protein and can be cleaved by proteinase K in solution if a GPI-linked protein is located and exposed at the outer leaflet of the spherical bleb or on the upper leaflet of bleb bilayer. In the assay, TIRF microscopy was used to monitor each YFP signal, and the signals were counted and tracked to establish the signal loss over time. The proteolytic cleavage of any accessible fluorescent domain of the GPI protein results the loss of fluorescent signal (YFP) in blebs and bleb bilayers when the cleaved

portion floats out of the evanescent field generated during TIRFM. As shown in **Fig. 5A**, control cases were the cell blebs without proteinase K treatment, where GPI-YFP signals remain unchanged over time (except for some photobleaching). However, with proteinase K treatment, blebs have prominent drops in GPI-YFP signals. The results indicate that GPI-YFPs are located on the outer leaflet of cell blebs and can be reached by protease in all blebbing conditions. In **Fig. 5B**, a very similar trend was observed in the planar bilayers made from the blebs, where the YFP signals remain the same in all control cases over time. Moreover, after adding proteinase K, the proteinase K cleaved most of the GPI-YFP in bleb bilayers and signals of GPI-YFP decreased significantly. These results show that in both cell blebs and bleb bilayers, the GPI-YFP protein orientation is maintained as in live cells. The FA/DTT exposure or serum starving methods do not affect the GPI-YFP protein orientation in both cell blebs and bleb bilayers.

These results imply blebs rupture as a "parachute," which keeps luminal sides downward facing the substrates when the bilayer forms,[37, 38] and that this mechanism seems to be preserved regardless of the concentration of chemical blebbing agent or serum starvation process used to generate the blebs. The parachuting rupture mechanism allows GPI-YFP in blebs to remain accessible to bulk solution after forming the bleb bilayer. Importantly, we note that although GPI-YFP orientation and rupture mechanism determined here was shown not to vary for these proteins as blebbing conditions changed, it is possible that this is not the case for every cell line and membrane protein.

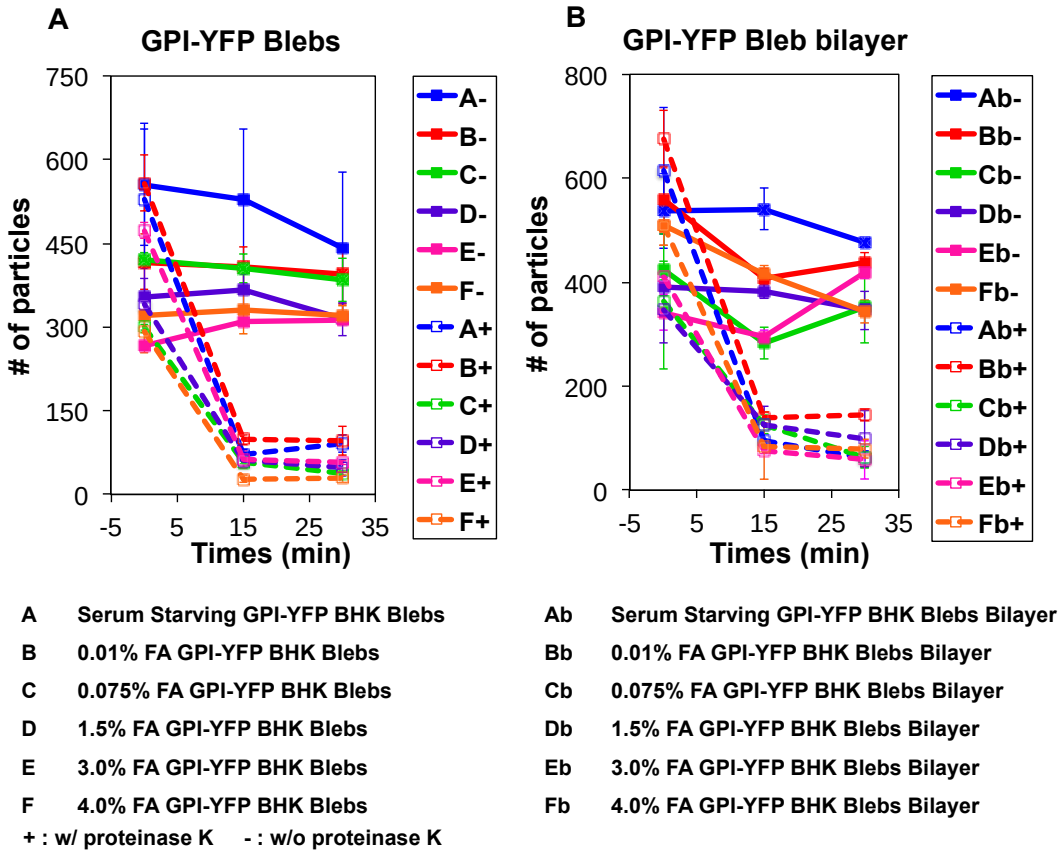

Figure 5. Protease cleavage assay for GPI-YFP orientation. (A) GPI-YFP protein orientation in the cell blebs was investigated by protease cleavage assay. At t = 0, Proteinase K was added to the blebs and cleaved all the accessible proteins. The signal drops indicate the GPI-YFP was accessible for proteases. (B) The bleb bilayer was treated using identical procedure as blebs, and a similar trend represents the protein preserved the orientation in cell blebs and cell bleb bilayer as in the cell membrane.

1.3.5. Characterizing the mobility and confinement of individual membrane proteins in planar bilayers using single particle tracking

After confirming protein orientation in bleb SLBs, protein mobility in them was assessed. Mobile proteins are essential for a biomimetic bilayer, but it is well documented that formaldehyde is a nonspecific crosslinking reagent and dithiothreitol reduces disulfide bonds and palmitoylated cysteines, which can impact phase partitioning.[17, 18, 19] The goal here was to assess the impact of these reagents on protein

mobility and protein confinement and compare against the case of serum-starving. Protein mobility was assessed using single particle tracking analysis by TIRF microscopy. For data analysis, a particle confined in an area smaller than the maximum displacement of fluorescent domain is regarded as immobile. Mean squared displacement (MSD) was used to determine the diffusivity of GPI-YFP. Moment scaling spectrum (MSS) analysis was use to reveal the confinement of GPI-YFP and heterogeneity of the plasma membrane.[32, 34] The particle is considered as confined if the value of parameter β is less than 0.4. In **Fig. 6A** and **B,** 0.075% FA GPI-YFP bleb bilayer shows maximums in mobility (at 90.9%) and diffusivity (at 0.83 $\mu m^2/s$). Compared to 0.075% FA condition, cells treated with less FA/DTT (serum starving, 0.01 %FA, 0.03 %FA) or higher concentrations (0.6 %FA, 1.5 %FA, 4 %FA) exhibited decreased mobility and diffusivity of GPI-YFP in bleb bilayers. In **Fig. 6C**, 0.075 % FA GPI-YFP bleb bilayer also exhibits the least confinement of GPI-YFP. Increasing or reducing FA/DTT from 0.075% FA conditions both leads to the *increase* of confinement of GPI-YFP. The results indicate the 0.075 %FA blebbing conditions leads to the maximum mobility and diffusivity of the protein, with minimum in protein confinement.

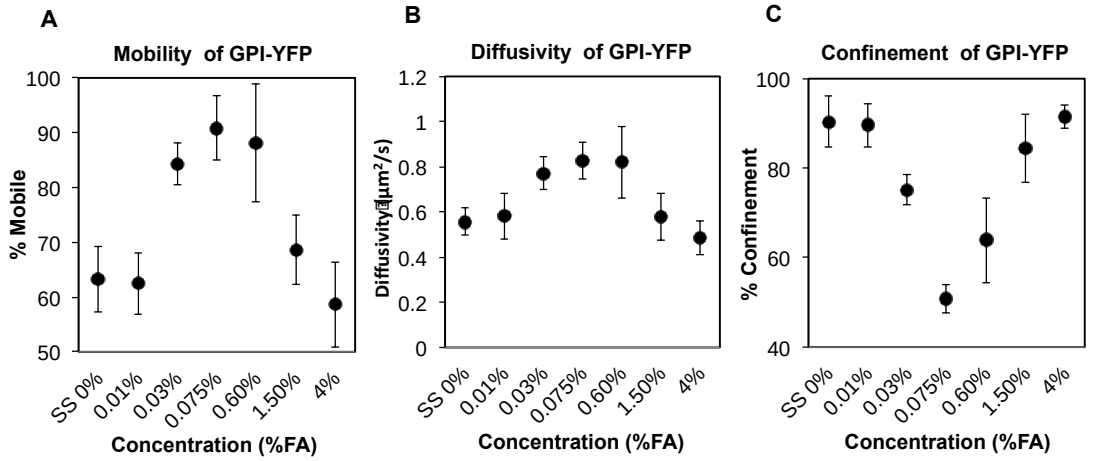

Figure 6. Single particle tracking for the motion of individual GPI-YFP protein. (A) Mobility of GPI-YFP in bleb bilayer formed by different kind of cell blebs. (B) Diffusivity of GPI-YFP in bleb bilayer. (C) Confinement of GPI-YFP in bleb bilayer.

There are several possible explanations for the observed trends in protein mobility, diffusivity, and confinement. For the higher FA/DTT concentrations, crosslinking and aggregation of protein may be one rationale for reduced mobility and diffusivity in bleb bilayers. Another plausible explanation is that the blebs are too stiff to rupture, resulting in a significant number of unruptured blebs on the surface. For the lower concentration blebbing agents, the explanation is not as straightforward. One plausible explanation is that the composition of lipid and protein of cell blebs varies as the concentration of chemical induction condition changes, which is supported to some degree by Western blot analysis (discussed later). For serum-starving, these blebs are the stiffest and so it is reasonable in that case that there would be the most unruptured blebs due to the higher energy required to form the planar structure. In the analysis that follows, more differences between serum-starvation generated blebs and the chemically-induced variety are revealed. It is the changes embodied in this difference that we believe is also reflected in the diffusion results observed here.

1.3.6. Characterization of lipid orientation in blebs and bleb bilayers

Until now, lipid orientation in these biomimetic platforms has not been assessed. To investigate the lipid orientation in cell blebs and bleb bilayers, we focused on phosphatidylserine (PS) lipids, as they are known to be asymmetric in the membrane and located on the inner leaflet in live cells and flip to the outer leaflet during early stages of apoptosis. In addition, by using fluorescently-labeled annexin V as a marker for PS, we can determine if PS lipids have inverted by binding of annexin V. This annexin V binding assay was used to probe the lipid orientation in blebbed cells, resultant blebs generated from those cells, and bleb bilayers formed from those blebs.

Annexin V was added to cultured BHK cells to determine the PS orientation in cells before and after the blebbing process with serum starving or chemical treatment. Before any treatment with blebbing solutions, the image shows that there is no annexin V binding on the surface for BHK cells, that is, the cell plasma membrane maintains PS lipid asymmetry **(Fig. 7A)**. However, after BHK cells were treated by either serum starving or 0.075% FA/DTT condition, annexin V was observed to bind to the cell surface indicating that PS lipid were now in the externally-facing leaflet **(Fig. 7B, C)**. BHK cells which were treated by serum starving method show the adhesion of annexin V to PS lipids, but the degree of PS lipid scrambling is apparently much less than the 0.075% formaldehyde treated condition. Additionally, the binding pattern of the serum starving case seems to be more localized (punctate), perhaps at sites where blebs were released, supporting that the mechanism of serum-starvation induced bleb release is different than chemically-induced blebs. In the chemically-

induced case, cells are slowly dying and so it stands to reasons that PS would be flipped to the other leaflet. Serum-starving seems to lead to another pathway, such as exocytosis, where cells are not yet dying, but shedding materials in response to the deficient media. Nonetheless, both chemical induction and serum starving cause PS lipids to flip to the outer leaflet of BHK cells, albeit to different degrees.

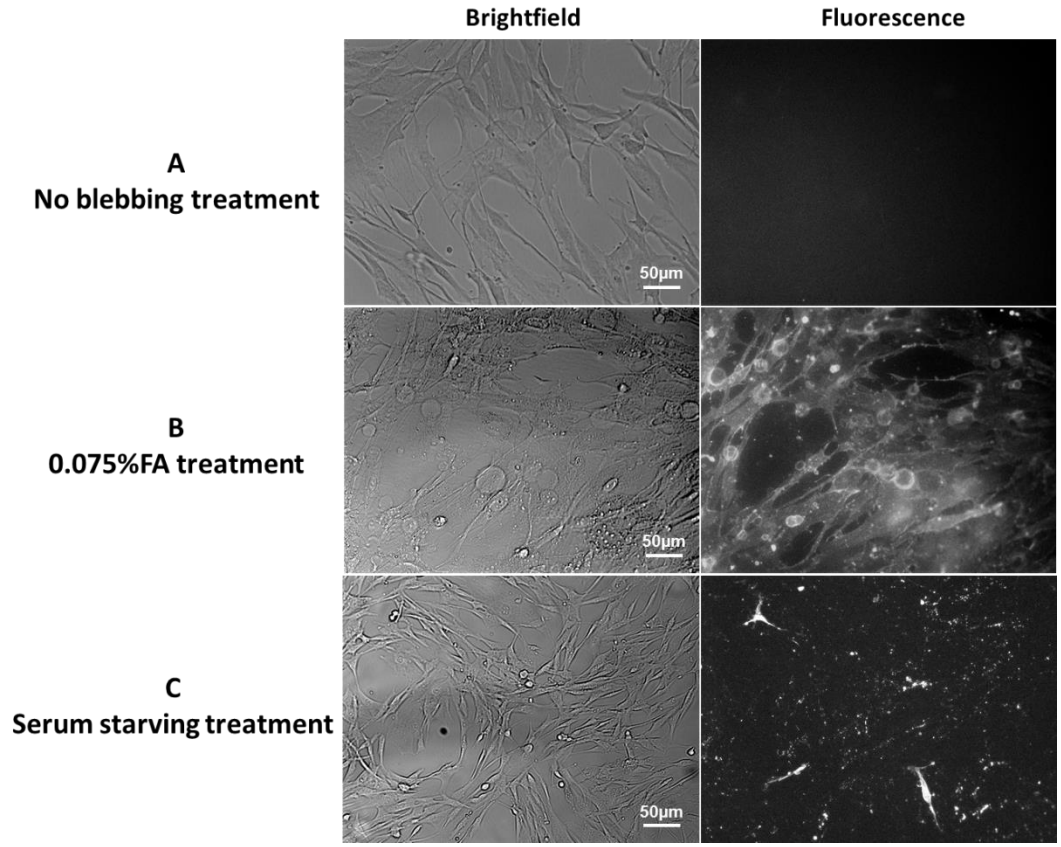

Figure 7. Annexin V assay for PS lipid orientation in BHK cells. (A) BHK cells before blebbing process were treated with annexin V. The BHK cells maintain PS asymmetry and show no annexin V binding to the surface of cells. (B) BHK cells after 0.075%FA exposure were treated with the annexin V shows substantial binding of annexin V. (C) BHK cells after serum starving method were treated with the annexin V and show less annexin V binding overall and more localized binding.

PS lipid orientation in cell blebs and bleb bilayers were characterized by annexin V assay as well to see if PS asymmetry was either maintained or lost. Plain POPC bilayer served as a negative control experiment and the image shows the annexin V does not bind to POPC bilayers **(Fig. 8A)**. 2% PS was mixed with 98% POPC which served as the positive control and the image shows that annexin V binds readily to a 2% PS lipid bilayer **(Fig. 8B)**. Blebs induced from both serum starving and 0.075% formaldehyde exposure were examined for PS lipid orientation. Cell blebs were adsorbed on the glass slides and the rest of the exposed glass substrate was blocked by BSA. Next, annexin V was added to probe the PS lipids orientation in blebs from both blebbing methods. In either serum starving or chemical exposure method, annexin V bound to the cell blebs, which indicates that the cell blebs also lost PS lipid asymmetry during blebbing **(Fig. 8C, E)**.

Given that cell blebs have already lost PS lipid asymmetry, we anticipated that the bleb bilayers would also lack PS lipid asymmetry. To test this, the annexin V assay was used to quantify bleb bilayer asymmetry. As expected, annexin V bound to the PS lipids in the bleb bilayers also **(Fig. 8D, F)**.

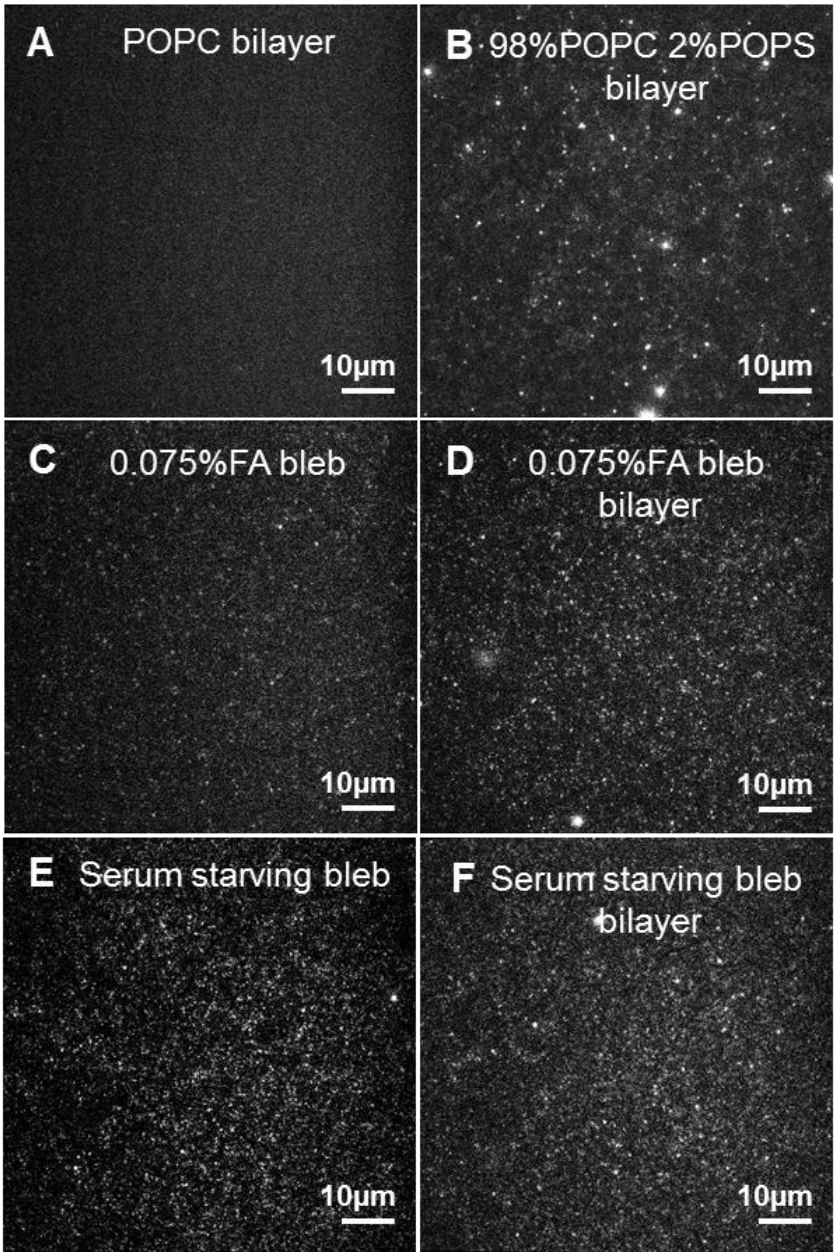

Figure 8. Annexin V assay for PS lipid orientation in cell blebs and bilayer. (A) POPC bilayer and (B) 98 %POPC 2 %POPS bilayer was used to indicate the annexin V only binds to the PS lipid. Cell blebs from 0.075 % FA exposure (C) and serum starving (E) reveal the cell blebs lost PS lipid symmetry. The bleb bilayers made from the cell blebs from 0.075 %FA exposure (D) and serum starving (F) indicate presence of PS lipid facing toward the bulk solution.

Apoptosis is a process of programmed cell death. PS externalization on the plasma membrane is the hallmark of apoptosis process.[28] As mentioned above, the blebbing process induced by both serum starving or chemical treatment leads to PS exposure in cells. In some sense this is not a surprising result, as the cells in these culture conditions are not thriving any longer. We also showed that PS is exposed on the outer leaflet in both cell blebs and bleb bilayer, but because the PS is already flipped in the cells, it is not possible to further distinguish by this assay if other lipid types are also flipping during bilayer formation or are already flipped. In the apoptotic situation, the first feature is PS externalization, which leads to phospholipid redistribution and induces apoptotic cell phagocytosis. The second feature is loss of cell volume, which leads to buckling of the membrane and shrinkage of cells, factors necessary for the formation of cell blebs.[39, 40] So, the apoptosis process and subsequent PS flip are intimately related to the process of generating the cell blebs. We do not know the extent of flip-flop of other lipids at this stage, nor if PS flip-flop is a valid universal indicator of loss of all lipid asymmetry in the bilayer. Unfortunately, few other assays are available to test other lipids of known asymmetry at this point in time.

Despite the PS exposure, the cell plasma membrane bleb bilayer importantly preserves the protein orientation and protein activity (described next), making this a beneficial platform for studying membrane protein function and activity and for use in a variety of *in vitro* applications.

1.3.7. Characterization of human aminopeptidase N enzyme activity in cell blebs

To evaluate the impact of blebbing conditions on protein activity, an enzymatic assay was performed on cell blebs expressing human aminopeptidase N (hAPN).

hAPN is a membrane-bound enzyme and H-Ala-AMC is the substrate for hAPN. As hAPN cleaves the substrate, the substrate becomes fluorescent. To be consistent across experiments, the concentration of cell blebs was measured by Nanosight and adjusted to 5×10^8 blebs/mL for each run, diluting and remeasuring concentration by Nanosight until the concentration target was reached. The cell blebs were then mixed with 270 mM H-Ala-AMC. Fluorescent signals were monitored and counted continuously by a fluorometer for 1.5 hours. As shown in **Fig. 9**, the concentration of FA/DTT used during blebbing impacts the activity of hAPN. The blebs induced by 0.01% FA shows the highest value of the fluorescence signal and the blebs induced by 4% FA shows the lowest value of the fluorescence signal. The activity of hAPN systematically decreases with increasing concentration of FA/DTT in blebbing solution. 4% was chosen as the upper limit, as this is the typical amount of formaldehyde used in cell fixation experiments. Interestingly, at this concentration, activity is almost completely lost, but mobility is not, indicating that crosslinking (via formaldehyde) is most likely occurring within the individual proteins itself (in this case apparently near the substrate binding pocket) rather than between two separate proteins, or that DTT has disrupted critical disulfide bonds near the pocket; in either case it is clear the higher the concentration of chemical inductant, the lower the protein activity. Given this trend, it was surprising to us was that the serum starved blebs were *not* the highest activity.

For the serum starving case, one plausible explanation for the drop in activity is that the mechanism of bleb formation is different from the chemical treatment and thus proteins may be in different states of maturation or glycosylation, for example,

when they are blebbed off. Evidence to support that the mechanism of bleb formation differs depending on bleb induction methods comes from the annexin V assay that shows different degrees of annexin V binding in BHK cells after different blebbing solution treatments. However, another possibility for the lower amount of activity is simply that protein content varies with blebbing induction method/conditions, *e.g.*, serum starved blebs have less enzyme content per concentration of blebs. Thus, we characterize protein expression level in the next section by conducting Western blots.

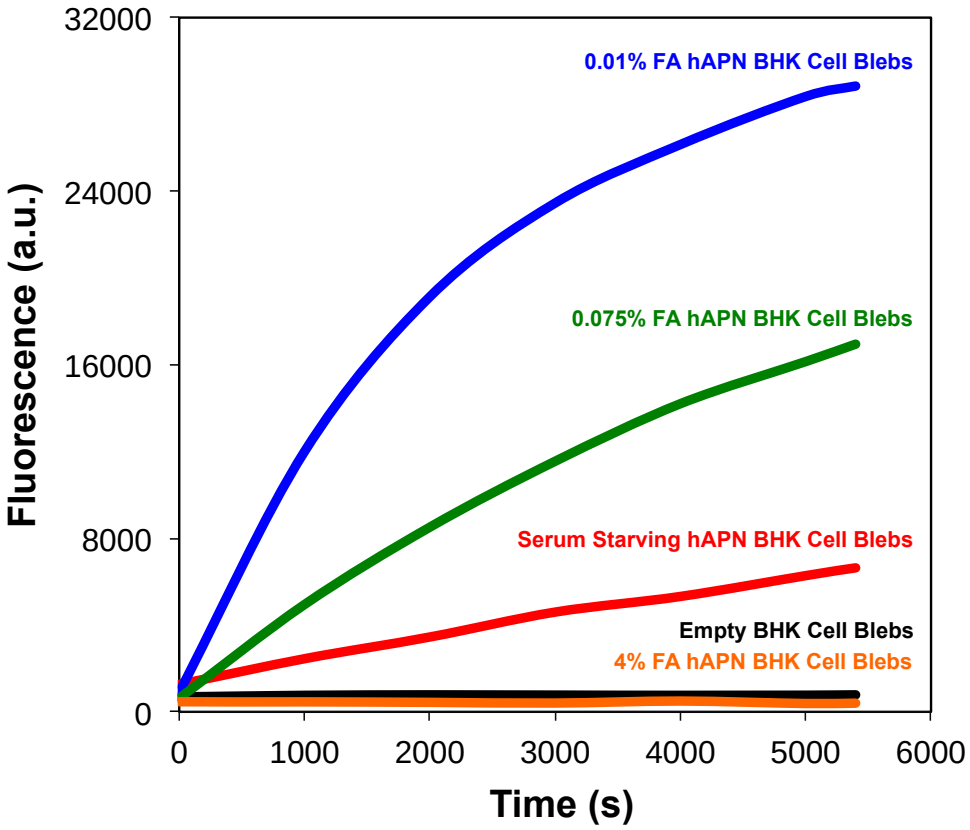

Figure 9. Human Aminopeptidase N Activity (hAPN) Assay. The activity of hAPN in cell blebs by various blebbing conditions was analyzed by enzymatic assay. The H-Ala-AMC is the substrate for hAPN. As the hAPN cleaves the H-Ala-AMC, the fluorescent signal releases. The activity of hAPN was probed by counting the fluorescent signal.

1.3.8. Impact of blebbing conditions on hAPN and GPI-YFP expression

The previous results on hAPN activity suggest that moderate to low FA treatments preserves more protein activity than the serum starving induction method, which does not correlate with the expectation that FA can crosslink proteins and DTT reduces disulfide bonds, and the expectation that these effects would reduce, not elevate, protein activity. Our initial hypothesis to explain this result was that protein expression levels must be reduced in the serum starving method relative to the FA/DTT induction method. Thus, to clarify how protein expression levels vary with blebbing treatments, cell blebs from various conditions were used to assess hAPN and GPI-YFP protein expression by Western blot. Cell blebs devoid of hAPN or GPI-YFP from the serum starving method were also analyzed by Western blot as negative control (N/C). To avoid batch to batch variability, concentrations of the cell blebs were determined by Nanosight and adjusted to identical concentrations.

In **Fig. 10A** and **10B**, Western blot results show bands of GPI-YFP (50 kDa) and hAPN (150 kDa), and cross-linked complexes of GPI-YFP (at 100 kDa) and hAPN (at 300kDa). To examine how expression level changes with variation in FA/DTT concentration, bands of GPI-YFP were detected and quantified as FA/DTT increased **(Fig. 10C)**. The results show that the protein levels of GPI-YFP decrease with the increasing concentration of FA/DTT in the blebbing solution most likely because of the crosslinking caused by formaldehyde. Interestingly serum starved blebs contain the *highest* protein level of GPI-YFP. Similarly, **Fig. 10D** shows that the protein levels of hAPN decrease with the increasing concentration of FA/DTT in blebbing solution and serum starving also yields the *highest* level of hAPN.

In the hAPN enzyme activity assay, the result indicates the activity of hAPN from serum starving method is only better than the 4% formaldehyde exposure case, but in the quantitative WB analysis of hAPN, it suggests the serum starved blebs contain the *highest* protein level of hAPN. This result further supports the hypothesis that the blebbing mechanism is different between serum starving bleb induction and formaldehyde exposure. One possibility is that the serum starving process may not only trigger the cell to generate the cell plasma membrane blebs but also exosomes.[41, 42] Thus in the serum starving method, these blebs may contain more non-functional, or immature, hAPN compared to chemically-induced method, which blister off directly from the plasma membrane. Even though the protein level in the serum starving method is the highest, the activity of hAPN in serum starving method is not consistent with the protein level.

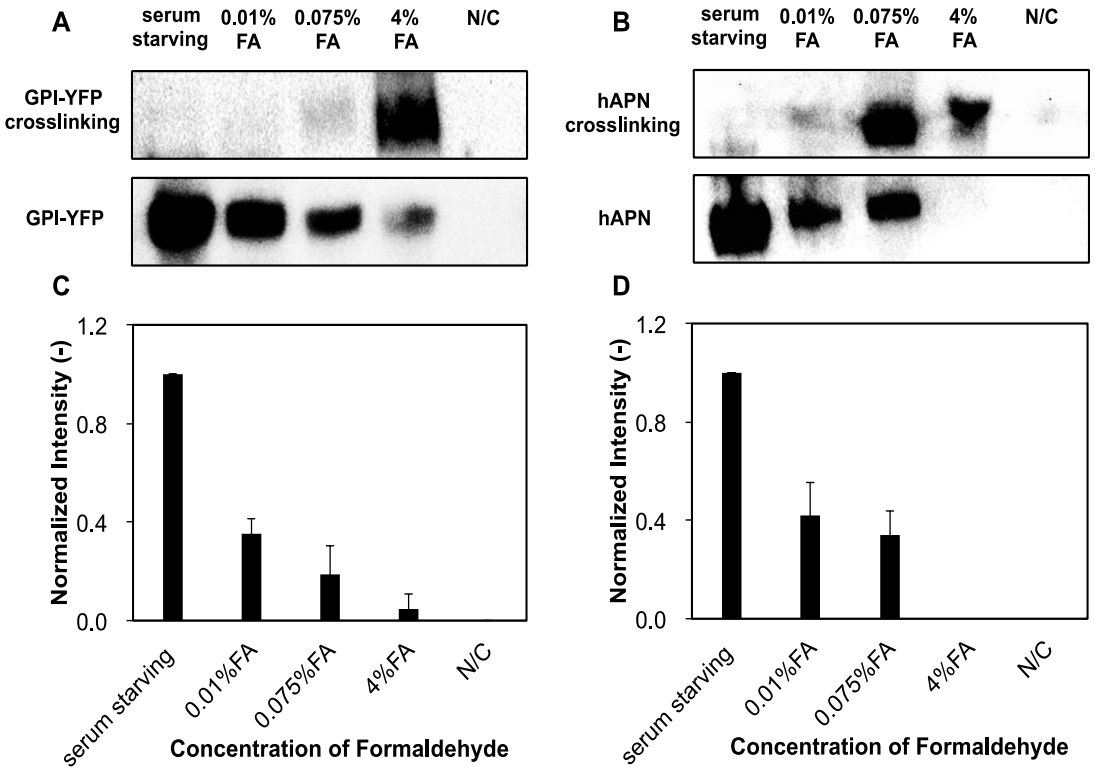

Figure 10. Western blot analysis for impact of formaldehyde on GPI-YFP and hAPN protein level. (A) Western blot for GPI-YFP blebs indicates the band of GPI-YFP and cross-linked complexes. (B) Western blot for hAPN blebs shows the band of hAPN and cross-linked complexes. (C) Quantitative analysis of GPI-YFP in western blot. (D) Quantitative analysis of hAPN in western blot.

1.3.9. Implications of this work

In this study, we characterized cell membrane blebs and bleb bilayers, which reveals the effects of the conditions used to induce blebbing on the protein, lipid, and proteoliposome properties. The results suggest that both induction methods, serum starving or chemical-induced, can impact the protein behavior in resulting cell blebs and bleb bilayers. Here we have identified conditions that promote proper protein orientation and the best protein fluidity and activity for these materials. The findings provide a well characterized template for studying protein-lipid, protein-protein, and

host-pathogen interactions in a biomimetic system that has many features of cell membranes. Furthermore, the general platform and characterization techniques can be expanded for studying other cell types (e.g. cancer cells, stem cells) with controllable conditions. In other words, these materials can be an advantageous *in vitro* model for mimicking *in vivo* cell surface reactions and/or controlling them for the study of phenomena in a variety of applications for biology and pathobiology research.

1.4. Conclusions

Planar cell membrane bilayers using cell blebs as an intermediate can be made from several cell lines.[13, 18, 43] Because of their planar geometry, the bilayer is compatible with a vast array of surface characterization tools. Key advantages of cell bleb bilayers is the ability to create them without the use of detergent or reconstitution, while maintaining the richness in composition of the cell membrane itself and the native protein orientation and activity. In this work, we characterized cell membrane properties from various blebbing methods/conditions and the impact on protein behavior in them. We show that GPI-YFP has the highest percentage of mobile proteins and least confinement in bilayers created from 0.075 %FA/DTT chemical induction. BHK cells exposed to bleb induction conditions display PS lipid externalization when exposed to either serum starving or chemical induction methods. Cell blebs and resultant bleb bilayers also lack PS lipid asymmetry. In the hAPN enzyme activity assay, we surprisingly found that cell blebs from 0.01 %FA exposure method give the highest enzyme activity, not cell blebs created from serum starving devoid of chemical inducers. However, Western blot analysis shows the serum

starving cell blebs express the most protein. From all this analysis, we conclude that the blebs that result from these two different induction methods are significantly different in various ways. This conclusion is further supported by cell bleb stiffness characterized by AFM, which reveals that serum starved blebs have the highest stiffness compared to any chemically-induced blebs. Taken together, we hypothesize that serum starved blebs are produced by a different mechanism that the chemically-induced blebs. One possibility is that serum starvation generates blebs via an exocytotic pathway, whereas the chemically-induced blebs can literally be observed to blister off from the plasma membrane. In conclusion, we believe this study clarifies conditions and promotes the usage of planar mammalian membrane platforms for emerging research topics like virus-host interactions or interactions between oncogenic microvesicles and cell surfaces.

1.5. Acknowledgements

The authors would like to thank Barbara Baird and David Holowka of Cornell University for providing the pYFP-GPI-N1 plasmid and Kathryn Holmes of University of Colorado for providing the pCI-neo-hAPN plasmid. This work was supported in part by the following grants to S.D.: National Science Foundation (CAREER grant CBET-1149452; CBET-1263701); Memorial Sloan Kettering Cancer Center U54CA199081 sub-award BD520101. H.G was supported in part by a NSF Research Experience for Undergraduates (sub-award of CBET-1263701).

Han-Yuan Liu, Hannah Grant, Hung-Lun Hsu, Raya Sorkin, Filip Bošković, Gijs Wuite and Susan Daniel. Planar Mammalian Membranes as Models of in vivo Cell Surface Architectures. Submitted to *ACS applied materials and interfaces,* 2017

CHAPTER 2

SINGLE PARTICLE TRACKING OF ONCOGENIC MICROVESICLE INTERACTIONS WITH PLANAR, SUPPORTED STEM CELL BILAYERS

2.1. Introduction

Sustained angiogenesis is a hallmark of breast cancer. Previous data suggests that breast cancer cell-derived microvesicles promote the differentiation of adipose derived stem cells into myofibroblasts.[44, 45] These myofibroblasts, in turn, stimulate tumor angiogenesis via increased proangiogenic factor section and extracellular matrix remodeling.[44, 45, 46] Thus, there appears to be a critical transfer of information from oncogenic microvesicles to stem cells that promotes their cellular transformation and the resulting biological outcome. However, the binding moieties of microvesicles and the mechanisms of triggering cargo release intra- and extracellularly remain unknown. Here, we use single particle tracking techniques to study the interactions of oncogenic microvesicles with stem cell surfaces. Because membrane binding and fusion are ubiquitous ways biomolecules are transported into cells and cellular compartments, our studies characterize these entry steps. A critical feature of this experiment is the development of planar stem cell bilayers, a platform which is compatible with a variety of characterization tools and microscopy methods. With this platform, we are able to monitor the binding and fusion of breast cancer derived microvesicles to chemically-tunable, planar bilayers mimicking stem cell surfaces. In this presentation, we describe this new approach to studies of oncogenic microvesicle entry and

delineate the effects of microvesicle-associated integrins and the properties of the extracellular environment on cancer microvesicle binding. Furthermore, single particle tracking was also used to define the mechanism of cancer microvesicle delivery of cargo via membrane fusion. The results indicate the impact of the microenvironment on the binding of cancer microvesicle and cargo delivery to adipose derived stem cells.

2.2. Materials and methods

2.2.1. Cell culture

Human Adipose-derived Stem Cells (ASCs) and MDA MB-231 human metastatic breast cancer cells (MDAs) were the gift from the Fischbach lab at Cornell University ASCs cultured in the corresponding growth media, ADSC-GM (Lonza). MDAs grown in Dulbecco's modified Eagle medium (DMEM) (CellGro) supplemented with 10% fetal bovine serum (Gibco), 100 U/ml penicillin and 10 μg/ml streptomycin (CellGro), 1% HEPES buffer (CellGro). Cultures were maintained in a 37 °C, 5% CO_2 incubator.

2.2.2. Preparation of liposomes

1-Oleoyl-2-palmitoyl-sn-glycero-3-phosphocholine (POPC) and 1,2-dipalmitoyl-sn-glycero-3-phosphoethanolamine-N-[methoxy(polyethylene glycol)-5000] (PEG5000-PE) were used in this experiment. Both are purchased from Avanti Polar Lipids. In the experiments, two formulations, pure POPC liposomes and 99.5% POPC 0.5% PEG50000-PE, were used to conduct the experiment. The liposomes were in the chloroform, and a stream of nitrogen was used to evaporate the chloroform

solvent gently. To ensure full evaporation, the lipid films were stored under the vacuum for 3 hours to remove the residual chloroform. To create vesicles, phosphate buffered saline (PBS) buffer (5mM NaH_2PO_4, 5mM Na_2HPO_4, 150mM NaCl at pH 7.4) was added to the dried films to the concentration of 2 mg/ml. Single unilamellar liposomes were prepared by extrusion using a 50 nm membrane at least 15 passes.

2.2.3. Preparation of plasma cell membrane blebs

6 ml of 1.5×10^6 cells/ml Human Adipose-derived Stem Cells (ASCs) were seeded in 10 cm perti dishes (Corning) and incubated for 24 hours in a 37 °C, 5% CO_2 incubator. After 24 hours, the cells were washed with GPMV buffer (2 mM $CaCl_2$, 10 mM HEPES, 150 mM NaCl at pH 7.4), and 4 ml of GPMV buffer with 25 mM formaldehyde (FA) and 2 mM dithiothreitol (DTT) (0.075%FA) was used to induce the cell blebs subsequently. The cells were incubated in the blebbing solution for 1 hour at 37 °C. After incubation for 1 hour at 37 °C, cell blebs were settled on ice for 15 min to separate cell debris and cell blebs were collected from supernatant.

2.2.4. Preparation for bleb planar bilayer

Polydimethylsiloxane (PDMS) wells were made by 10:1 elastomer/crosslinker mixture of Sylgard 184 (Robert McKeown Company) and baked for 5 hours at 78°C. PDMS wells were attached to the dry clean glass slides (25×25mm No.1.5, VWR). The glass slides were pretreated by piranha solution (70% (v/v) H_2SO_4 (BDH) and 30% (v/v) H_2O_2 (Sigma 50 wt %)) for 10 min and rinsed by flushing DI water 20 min continuously. Then 100 μL of solution containing blebs at approximately 5×10^8 blebs/mL was added into the well and incubated for 15 min. After incubation, the well was rinsed gently with PBS buffer to remove the unattached blebs. The 100 μL

liposomes at 2 mg/mL was added into the well continuously and incubated for 30 min to form the bleb bilayer. After the bleb bilayer formed, the well was rinsed with PBS buffer again to remove the excess liposomes.

2.2.5. Adipose Derived Stem Cell Bleb Bilayer Formation for Fluorescence Microscopy.

Adipose derived stem cell blebs were induced by 0.075%FA exposure method as the above procedure. In order to verify the rupture of blebs, Octadecyl Rhodamine B chloride (R18, Molecular Probes), a membrane intercalating fluorophore, was used to label the cell blebs membrane, and nonintegrated R18 was removed by using the G25 spin column (GE Healthcare) before incubating in the PDMS well. After formed the bilayers, the bilayers were scratched to assist in focusing the bilayer and maintaining the same z-plane during time lapse experiments. The process of bleb rupture was recorded by inverted Zeiss Axio Observer.Z1 microscope with α Plan-Apochromat 40× objectives. Diffusion of bilayer was characterized by fluorescence recovery after photobleaching (FRAP). A spot with 20 μm diameter in bilayer was bleached by 4.7 mW 488 nm krypton/argon laser for 200 ms. The recovery of bleached spot was monitored for 15 min and the fluorescence intensity of spot was determined after normalization in each image. The data of fluorescence intensity was fit into Bessel function following the method of Soumpasis et al.[47] and then the following equation, $D=w^2/4t_{1/2}$, where w is the full width at half-maximum of the Gaussian profile of the focused beam, was used to calculate the diffusion coefficient.

3.2.6. Antibody Binding to Confirm the Component of ASCs in the Supported Bilayer

POPC bilayer or 99.5%POPC 0.5% PEG5000-PE bilayer was blocked with the 100 μl 20% goat serum, and then incubated with 100 μl 1:100 anti-integrin beta 1 (R&D Systems) for 1 hr. The unbound primary antibody was rinsed out and 100 μl 1:500 of Alexa Fluor 568 conjugated-goat anti-mouse IgG secondary antibody (Molecular Probes) was added and incubated for 1 hr. Then, the excess secondary antibody was rinsed out and the sample was imaged with the inverted fluorescence microscope, the setting and operation described below. ASCs/POPC bilayer and ASCs/99.5%POPC 0.5%PEG5000-PE bilayer were treated by the same procedure but without the primary antibody to verify the nonexistence of nonspecific binding from secondary antibody. ASCs/POPC bilayer and ASCs/99.5%POPC 0.5%PEG5000-PE bilayer were treated by the same procedure as POPC bilayer to verify the integrin beta 1 binding. The setting of microscope was described latter.

2.2.7. Cancer microvesicle isolation

MDAs were maintained in their growth media until 80–90% confluency and then changed the growth media to 30 ml of serum-free Dulbecco's modified Eagle medium (DMEM) (CellGro) supplemented with 100 U/ml penicillin and 10 μg/ml streptomycin (CellGro). After 7-12 hours, the media was collected into a fresh 50 ml tube and centrifuged two times to remove the cell debris. Then, microvesicles were isolated by 100,000 MWCO concentration filter centrifugal tubes (Millipore).

2.2.8. Microvesicle interaction with stem cell planar supported bilayer

Pure POPC bilayer, 99.5%POPC 0.5% PEG5000-PE bilayer, ASCs/POPC bilayer and ASCs/99.5%POPC 0.5%PEG5000-PE bilayer were used in this experiment. Octadecyl Rhodamine B chloride (R18, Molecular Probes), a membrane

intercalating fluorophore, was used to label the cancer microvesicle, and nonintegrated R18 was removed by using the G25 spin column (GE Healthcare). The cancer microvesicles incorporated with R18 were incubated in the well for 20 mins and then the unbound microvesicles were rinsed out by PBS buffer. The images of microvesicles binding were recorded by total internal reflection fluorescence microscopy. The microscope setting and operation will be described later.

2.2.9. Impact of integrin beta 1 for microvesicle binding

Stem cell planar supported bilayer was blocked by 20% goat serum and then incubated with cancer microvesicles for 20 mins. The unbound cancer microvesicles were rinsed out by PBS buffer. Stem cell planar supported bilayer was blocked by 20% goat serum and then incubated with anti-integrin beta 1 at the concentration of 1:100 for 1 hr. After incubation of antibody, the cancer microvesicles were added into the well. After 20 mins, the unbound microvesicles were rinsed out by PBS buffer. The image process and microscope setting will be described in a later section.

2.2.10. Fabrication of microfluidic device

The generation of microchannel silicon mold developed using soft lithography was published previously.[15, 48] The pattern contains six trenches which dimensions are 70 μm deep, 135 μm wide and 1.5 cm long with 100 μm spacing between each channels. Polydimethylsiloxane (PDMS) were made by 10:1 elastomer/crosslinker mixture of Sylgard 184 (Robert McKeown Company) and coated on the silicon mold. The PDMS was baked for 3 hr at 78°C. The glass slides and microfluidic device were treated with oxygen plasma using a Harrick Plasma Cleaner at a pressure of 750

millitorr on the “high” setting for 15 s. The glass slide and microfluidic device were then assembled together gently and annealing was performed at 78°C for 15 min.

2.2.11. pH trigger cancer microvesicle fusion

The ASCs/99.5%POPC 0.5%PEG5000-PE bilayer was incubated with cancer microvesicles incorporated R18 for 20 mins and then the unbound microvesicles were rinsed out by GPMV buffer. The pH was reduced from 7 to 3. The fusion events were observed and recorded by total internal reflection fluorescence microscopy.

2.2.12. TIRF Microscope Setting and Operation

The antibody binding for ASCs bilayer, microvesicle binding experiments, and microvesicle fusion experiments were conducted by using total internal reflection fluorescence (TIRF) microscopy on an inverted Zeiss Axio Observer.Z1 microscope with an α Plan-Apochromat 100× objective. 488 nm and 561 nm wavelength from solid-state lasers were used to excite the sample. A Laser TIRF 3 slider (Carl Zeiss, Inc.) was used to control angle of incidence at ~68° generating the evanescent wave around 100 nm and total internal reflection. The excitation light was filtered by Semrock LF488-B-ZHE filter cube and sent to the electron multiplying CCD camera (ImageEM C9100-13, Hamamatsu).

2.3. Results and discussion

2.3.1. Adipose Derived Stem Cell Bleb Bilayer

Using the 0.075% FA exposure method, we created the adipose derived stem cell blebs. Then, using the adipose derived stem cell blebs as the intermediate to form the stem cell bleb bilayer, we verified the rupture of these blebs and visualized the

formation of the stem cell bleb bilayer using octadecyl rhodamine (R18), a membrane intercalating fluorophore, that was doped into stem cell blebs. Initially, the R18 signal was confined in the adsorbed stem cell blebs, prior to rupture (Figure 1A). The dark mechanical scratch at the lower right corner was made to verify the consistency of the focus plane during image acquisition. As the fusogenic vesicles, POPC liposomes, were added into the well, the adsorbed stem cell blebs were triggered to rupture and form the stem cell bleb bilayer. During this formation process, the fluorescent images show the diffusion of R18 as the R18 spreads out relatively uniformly within the planar bilayer (**Figure 1A**). After formation, fluorescence recovery after bleaching (FRAP) was used to determine the fluidity of the planar SLB and verify the R18 was no longer confined in the cell blebs but moving in the planar supported bilayer. In this technique, the laser beam was used to form the 20 μm diameter spot in the R18 labeled supported bilayer. As shown in Fig. 8B, the plot is a typical fluorescence recovery of R18 in the stem cell planar supported bilayer. The plot indicates the recovery is nearly restored to 90%. Note that the recovery curve is continuous and fits the diffusion model well. The diffusion coefficient of the stem cell planar supported bilayer is 0.196 ± 0.005 $\mu m^2/s$.

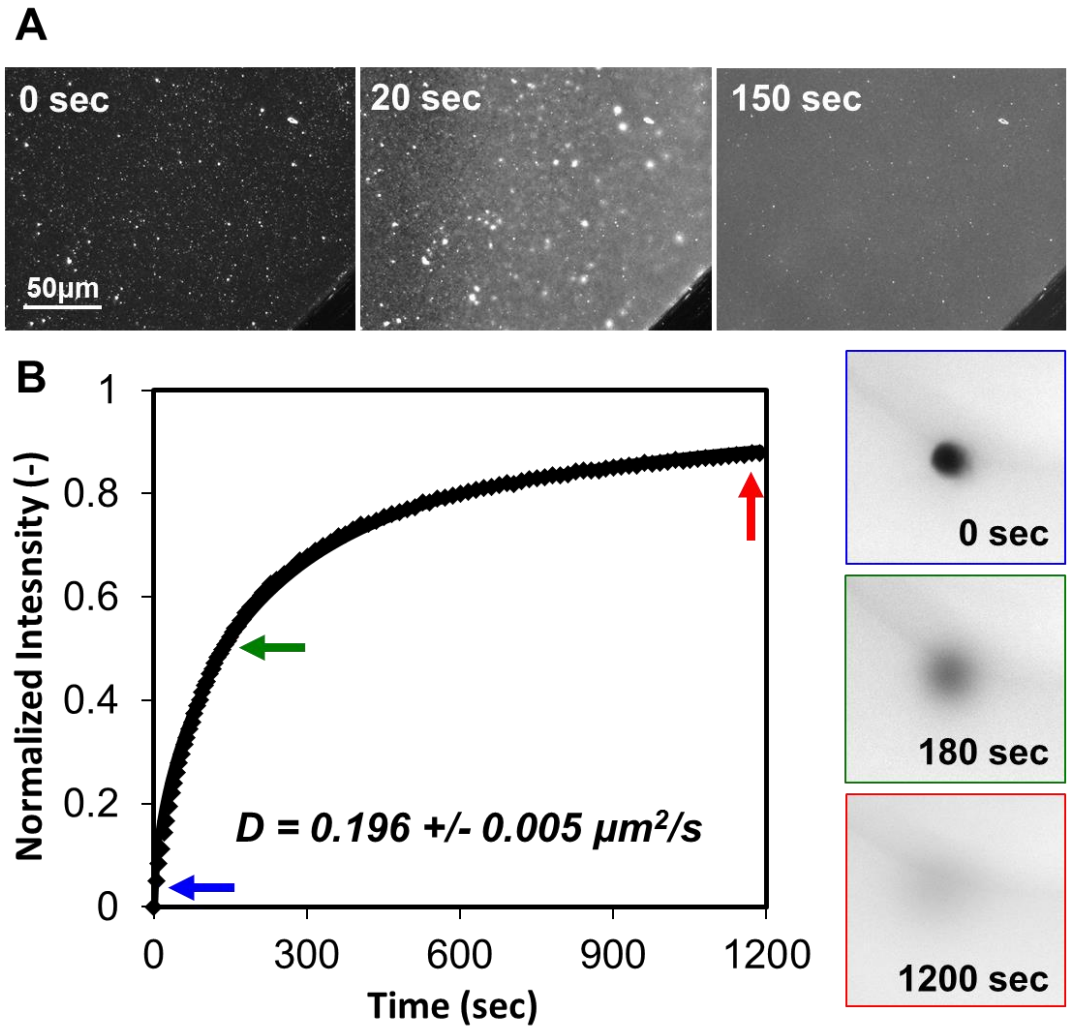

Figure 1. Adipose derived stem cell bleb bilayer formation and mobility. (A) Adipose derived stem cell blebs containing R18 adsorbed to the glass slides. Then, the POPC liposome solution not containing the R18 was added to the adsorbed blebs. All fluorescent signals come from release of R18 initially trapped in cell blebs before rupture. After adding the POPC liposomes, adipose derived stem cell bleb bilayer formation observed for 150 sec. (B) R18 fluorescence recovery after bleaching in the adipose derived stem cell bleb bilayer. The spot was bleached with a 561 nm laser beam. The diameter of the spot is about 20 μm. Each color-coded arrow on the plot corresponds to the each image of fluorescence recovery after bleaching. The diffusion coefficient on the plot is the average number from several experiments.

2.3.2. Antibody Binding to Confirm the Component of ASCs in ASCs/POPC bilayer

To confirm the essential component of adipose derived stem cell was incorporated into the planar supported bilayer, anti-integrin beta 1 antibodies and Alexa Fluor 568 conjugated-goat anti-mouse IgG secondary antibodies were used to verify the presence of stem cell marker, integrin beta 1, in it. As shown in the **Fig. 2A**, a POPC bilayer is the control experiment. The POPC bilayer was incubated with goat serum for blocking. After incubation, the POPC bilayer was incubated with anti-integrin beta 1 antibodies. Next, the POPC bilayer was rinsed with PBS buffer to remove excess antibodies. Then, the POPC bilayer was treated with the Alexa Fluor 568 conjugated-goat anti-mouse IgG secondary antibodies. The excess antibodies were removed by rinsing the PBS buffer. The results show that there is minimal antibody binding in the POPC bilayer. In **Fig. 2B**, an ASCs/POPC bilayer was treated with the same procedure but without the anti-integrin beta 1 antibodies incubation to assess the affinity of the secondary antibody for the stem cell bilayer. The image of sample 2B shows no antibody binding and indicates nonexistence of nonspecific binding from Alexa Fluor 568 conjugated-goat anti-mouse IgG secondary antibodies. As **Fig. 2C** shows, when the ASCs/POPC bilayer was treated with the same procedure as POPC bilayer, a significant amount of specific antibody binding occurs on the stem cell bleb bilayer. The specific binding indicates not only the integrin beta 1 proteins were present in the stem cell bleb SLB, but also a significant amount of integrin beta 1 was facing the bulk solution, in alignment with all our previous studies confirming that the blebs rupture as parachutes and result in “outside-up” proteins. As a mimetic cell plasma membrane platform, adipose derived stem cell bleb SLB not only

incorporate the component of adipose derived stem cell, integrin beta 1, but also imitates the orientation of integrin beta 1 as adipose derived stem cells.

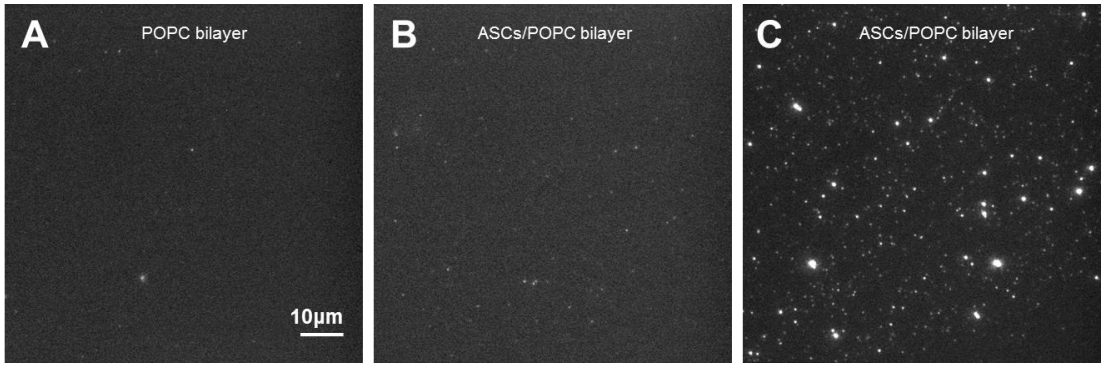

Figure 2. Antibody binding to confirm the component of adipose derived stem cell in ASCs/POPC bilayer. (A) POPC bilayer was used to show no binding from the anti-integrin beta 1 and Alexa Fluor 568 conjugated-goat anti-mouse IgG secondary antibody in only POPC bilayer. (B) ASCs/POPC bilayer was treated with the same steps but without adding the anti-integrin beta 1 antibodies. The image shows no nonspecific binding from Alexa Fluor 568 conjugated-goat anti-mouse IgG secondary antibodies. (C) ASCs/POPC bilayer was used to indicate the specific binding from anti-integrin beta 1 antibodies and Alexa Fluor 568 conjugated-goat anti-mouse IgG secondary antibodies.

2.3.3. Antibody Binding to Confirm the Component of ASCs in ASCs/99.5%POPC 0.5%PEG5000-PE bilayer

In **Fig. 3A** and **3C**, 99.5 %POPC 0.5 %PEG5000-PE bilayer and ASCs/99.5 %POPC 0.5 %PEG5000-PE bilayer were treated with the same procedure as the pure POPC bilayer. The images indicate no primary and secondary antibody binding in 99.5 %POPC 0.5 %PEG5000-PE bilayer, but shows binding in ASCs/99.5 %POPC 0.5 %PEG5000-PE bilayer. The results indicate the integrin beta 1 proteins were incorporated into ASCs/99.5 %POPC 0.5 %PEG5000-PE bilayer. As shown in **Fig. 3B**, ASCs/99.5 %POPC 0.5 %PEG5000-PE bilayer treated with the same procedure, but without the anti-integrin beta 1 antibodies incubation, shows no antibody binding

and indicates nonexistence of nonspecific binding from Alexa Fluor 568 conjugated-goat anti-mouse IgG secondary antibodies. The results indicate the integrin beta 1 proteins were incorporated into stem cell supported lipid bilayer and significant amount of integrin beta 1 proteins was also facing the bulk solution.

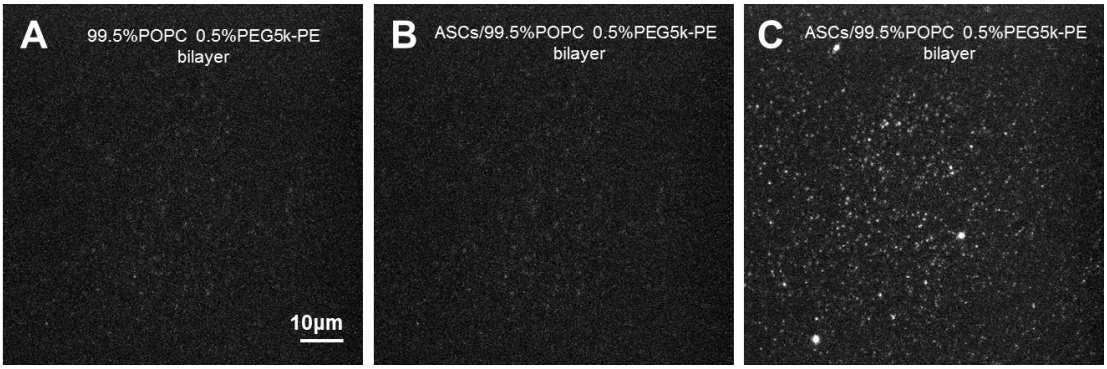

Figure 3. Antibody binding to verify the component of adipose derived stem cell in ASCs/99.5%POPC 0.5%PEG5000-PE bilayer. (A) 99.5%POPC 0.5%PEG5000-PE bilayer was used to show no specific binding from both primary and secondary antibody. (B) ASCs/99.5%POPC 0.5%PEG5000-PE bilayer was treated with the same steps but without adding the anti-integrin beta 1 antibodies. The image indicates nonexistence of nonspecific binding from secondary antibody. (C) ASCs/99.5%POPC 0.5%PEG5000-PE bilayer was used to indicate the specific binding and confirm bilayer incorporate ASCs components.

2.3.4. Microvesicle interaction with stem cell planar supported bilayer

MDAs microvesicles were labeled by Octadecyl Rhodamine B chloride (R18, Molecular Probes), a membrane intercalating fluorophore. Total internal reflection microscopy (TIRF) was applied to observe the cancer microvesicles binding in various bilayer. Cancer microvesicles were added into well and incubated. The excess and unbound microvesicles were removed by PBS buffer. Surprisingly, MDAs microvesicles can bind to pure POPC bilayer **(Fig. 4A)**. Because the bilayers incorporate the component of ASCs from ASCs blebs, the MDAs microvesicles bind to the ASCs/POPC bilayer **(Fig. 4B)** and ASCs/99.5 %POPC 0.5 %PEG5000-PE

bilayer **(Fig. 4D)** as expected. For 99.5 %POPC 0.5 %PEG5000-PE bilayer **(Fig. 4C)**, MDAs microvesicles binding does not occur as shown in the image.

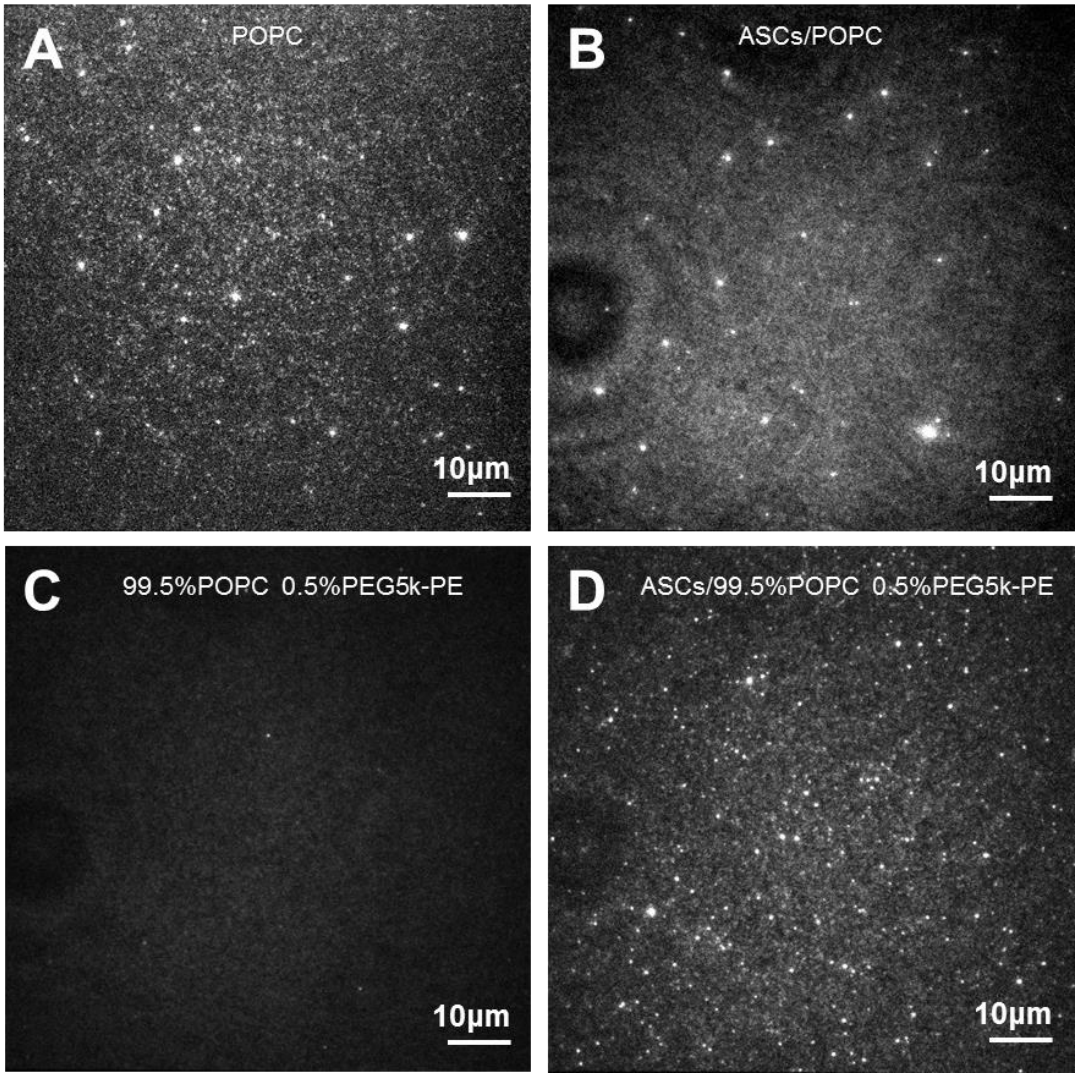

Figure 4. MDAs microvesicles binding in bilayer (A) POPC bilayer exists the MDAs microvesicles binding. (B) ASCs/POPC bilayer shows the binding of MDAs microvesicle. (C) 99.5% POPC 0.5%PEG5000-PE bilayer shows nonexistence of MDAs microvesicles binding. (D) ASCs/99.5% POPC 0.5%PEG5000-PE bilayer shows the binding of MDAs microvesicles.

2.3.5. Effect of integrin beta 1 for microvesicle binding

To confirm the specific effect of integrin protein on the cancer microvesicle binding, the anti-integrin beta 1 was used to block the integrin beta 1 protein as a

means to interrupt this binding. The stem cell SLB was blocked by goat serum for 1 hour and then incubated with anti-integrin beta 1 for 1 hour. ASC/POPC bilayer without integrin beta 1 blocking **(Fig. 5A)** shows much more microvesicle binding compared to ASCs/POPC bilayer with integrin beta 1 blocking **(Fig. 5B)**. In ASCs/99.5 %POPC 0.5 %PEG5000-PE bilayer case, ASCs/99.5 %POPC 0.5 %PEG5000-PE bilayer without integrin beta 1 blocking shows significant microvesicle binding **(Fig. 5C)**. However, ASCs/99.5 %POPC 0.5 %PEG5000-PE bilayer with integrin beta 1 blocking shows much less microvesicle binding **(Fig. 5D)**. The results reveal the effect of integrin beta 1 for microvesicle binding. In the both blocking case, the images indicate the bilayer significantly reduced microvesicle binding. Integrin beta 1 protein therefore appears toplay an important role for microvesicle binding.

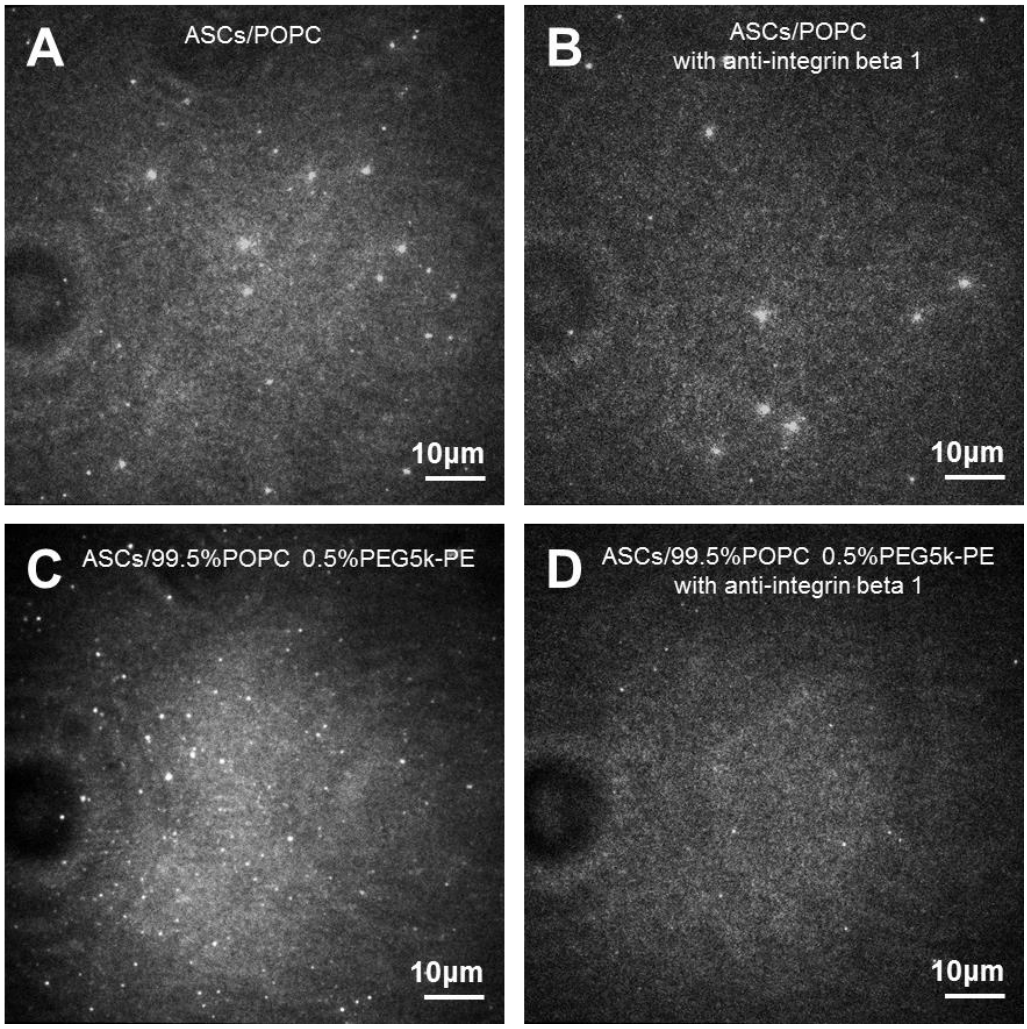

Figure 5. Effect of integrin beta 1 for microvesicle binding. (A) ASCs/POPC bilayer without antibody blocking for integrin beta 1. (B) ASCs/POPC bilayer with antibody blocking for integrin beta 1. (C) ASCs/99.5%POPC 0.5%PEG5000-PE bilayer without antibody blocking for integrin beta 1. (D) ASCs/99.5%POPC 0.5%PEG5000-PE bilayer with antibody blocking for integrin beta 1.

2.3.6. pH triggering of cancer microvesicle fusion at single particle level

Microvesicles are known to mediate the cell-cell communication. Microenvironment may, in turn, influence the entry and release of cancer microvesicle.[49] Here, the impact of pH on cancer microvesicles fusion was investigated by single particle tracking technique.[50] To monitor cancer microvesicles entry and fusion at the single particle level, individual microvesicle fusion events were

recorded by using total internal reflection fluorescence (TIRF) microscopy. R18 was used to label cancer microvesicles and carry out the cancer microvesicles fusion experiment. ASCs/99.5 %POPC 0.5 %PEG5000-PE bilayer was incubated with MDAs microvesicles for 20 min at pH 7. The unbound MDAs microvesicles were removed by PBS buffer. Here, the binding of MDAs microvesicles were observed in the stem cell SLB. The MDAs microvesicles labeled with R18 fuse with stem cell SLB after triggering with pH 3.0 **(Fig. 6)**.

The results indicate that pH plays an important role for cargo release of cancer microvesicles. However, Mechanism of cargo release of cancer microvesicles is still far from clear. The characterization of pH triggering microvesicle fusion is still needed to reveal the detail of pH to cancer microvesicles entry and fusion.[51, 52] Total internal reflection microscopy was used to measure each fusion events and collect the data of fusion lag time, pore formation time. These data will be fit into the model and reveals the detail of fusion rate constant and intermediate steps in the fusion pathway.

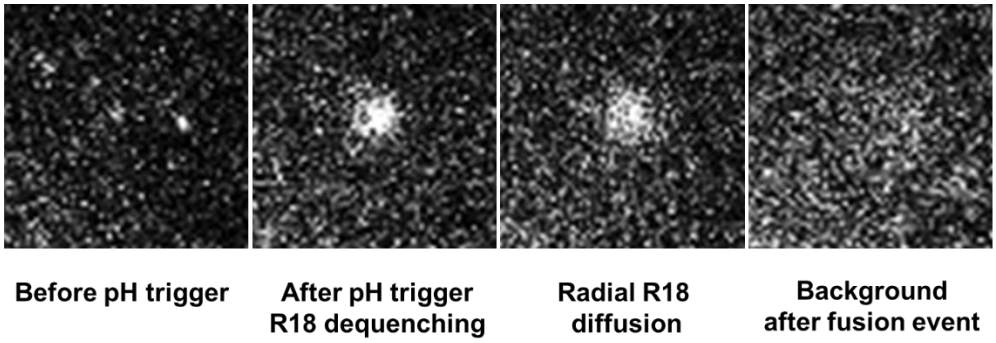

Figure 6. pH trigger cancer microvesicle fusion at single particle level. The MDAs microvesicles were labed with R18 and bind to the stem cell SLB. After triggering with pH 3.0, MDAs microvesicles fused with stem cell SLB. R18 dequenched and radially diffused away from fusion site.

2.3.7. Implications of this work

In our study, we verified the formation and fluidity of stem cell SLB. The antibody binding also revealed specific binding to integrin beta 1 protein and confirmed the component of ASCs in the stem cell SLB. Because the binding moieties of microvesicles and the mechanisms of triggering cargo release are not clear, this biomimetic platform can be applied to study the impact of microenvironmental factors (calcium, pH, etc.) on microvesicles binding with and entry through stem cell membrane surfaces. The formation of stem cell supported lipid bilayer using the blebbing technique opens the possibility for quantitative characterization of cancer microvesicles binding and fusion.

2.4. Conclusions

In this work, blebbing technique was used to form the stem cell SLB. Because of the planar geometry, stem cell SLB is compatible with a variety of surface characterization tools such as total internal reflection fluorescence (TIRF) microscopy. In our study, we proved the formation of stem cell SLB and revealed the fluidity of this biomimetic platform. Besides, anti-integrin beta 1 was used to confirm the stem cell SLB incorporate the component of ASCs. Here, we also applied this platform to investigate the cancer microvesicles interaction with stem cell surface. We show the cancer microvesicles can bind to not only the stem cell SLB but also the pure POPC bilayer. Stem cell SLB blocked by anti-integrin beta 1 shows the dramatic reduce of microvesicle binding in bilayer. This result reveals the integrin beta 1 protein may play the important role for cancer microvesicles binding. Furthermore, the cancer microvesicles fusion with stem cell SLB was observed by total internal reflection fluorescence (TIRF) microscopy after pH triggering.[51, 52] In conclusion, we believed

this work presents a novel biomimetic platform, stem cell SLB, to study the interaction between oncogenic microvesicle and stem cell. This biomimetic platform allows us to study the microvesicles binding and mechanism of cancer microvesicle delivery of cargo via membrane fusion, and opens an efficient way to characterize the cancer microvesicle binding and fusion at the single particle level.

2.5. Acknowledgements

This work was supported in part by the following grants to S.D.: National Science Foundation (CAREER grant CBET-1149452; CBET-1263701); Memorial Sloan Kettering Cancer Center U54CA199081 sub-award BD520101.

Han-Yuan Liu, Johana Uribe, Lakshmi Nathan, Claudia Fischbach-Teschl, Susan Daniel. Single particle tracking of oncogenic microvesicle interactions with planar, supported stem cell bilayers. 2017

CHAPTER 3

FUTURE DIRECTION

3.1. Dynamic Interaction between Cancer microvesicle and Stem Cell

Microvesicles are small vesicles released by donor cells and can be taken up by recipient cell. Recently, the advances in study of microvesicle reveal that microvesilces play the important role in cell to cell communication. Bioactive cargo of microvesicles, included RNA, microRNA, DNA, and protein, can have significant impact on phenotype of recipient cells. However, the binding and entry of microvesicle are still not well understood. Further research is needed to understand precise mechanism how microvesicle entry to the cells. Our previous study indicates the planar stem cell bilayer is a potential way to open the new insights for studying the interaction of cancer microvesicle and stem cell surface.

3.1.1. Quantify microvesicle binding and dependence on integrin-fibronectin interactions

It has been proposed that integrin beta 1 facilitate interaction of microvesicle with extracelluar matrix[50] and our previous work also reveals the integrin beta 1 may play the important role on microvesicle binding with stem cell surface. We can adjust the amount of bleb material and so amount of intergrins in our planar stem cell bilayer. The impact of integrin on microvesicle binding can be quantitative analyzed. We will also separately conduct antibody binding experiment to quantify the amount of integrin in planar stem cell bilayer. The single particle tracking technique will be used

to measure the resident time of microvesicle binding and then we can characterize the binding interaction through binding rate, binding strength, and avidity.

3.1.2. Define mechanism of microvesicles delivery of cargo via membrane fusion

In our previous results, the cancer microvesicle fused with planar stem cell bilayer after pH triggering. Our prelim data indicates pH plays the important role for entry of cancer microvesicle with stem cell. But, it is far from clear to well understand the mechanism of cargo release of cancer microvesicle. The other triggers included calcium spike, and endosomal proteases will be examined. Here, we will combine the microfluidic device to conduct our experiment which will be simple to control and mimic the microenvironmental condition. The single particle tracking technique will be used to observed each fusion events and collect the data of fusion lag times, pore formation times, and lipid mixing. These data will be fit to models to obtain fusion rate constants and details about intermediate steps in the fusion pathway.

3.2. Charge Induced Formation of Planar Plasma Membrane on PMETAC Substrate

In our previous results, the cell plasma membrane blebs are negative charge. We will apply the charge attractive force to induce the cell plasma membrane blebs rupture and form the bilayer without adding any liposomes. Poly([(2-methacryloyloxy)ethyl]trimethylammonium chloride) (PMETAC) is the polymer with permeant positive charge.[53] Because PMETAC brush has following properties such as hydrophilic, low roughness, high water retention and bio-compatible, PMETAC brush will be grown on the glass slides and induce the formation of bilayer from only cell

plasma membrane blebs via charge attractive force between PMETAC and cell plasma membrane blebs itself. The other potential advantage of this system is brush structure of PMETAC which could be the cushion between the bilayer and glass slides, avoid the interaction between transmembrane protein and glass slides, and preserve the mobility of transmembrane protein. We aim to create the biomimetic platform with one-side cushion and without adding liposomes. We will study the impact of grafting density of PMETAC, which related to charge density, on plasma membrane bilayer formation and the rupture orientation of cell blebs. After well understanding the impact of PMETAC on bilayer formation, we will move on to study the protein behavior such as diffusion and orientation in this novel platform.

Han-Yuan Liu, Wei-Liang Chen, Christopher K. Ober, Susan Daniel. Molecularly-Complete Planar Supported Cell Plasma Membrane Combining Polyelectrolyte Brushes as Cushion. 2017

CHAPTER 4

CONCLUSIONS

To create a closer mimic of cell membranes, there is increasing interest to create the SLB directly from plasma cell membrane vesicles, blebs, which are native membrane vesicles and can be generated by either chemical-free or chemical-induced method. Because of cholesterol content, lipids diversity, and proteins density in plasma cell membrane vesicles, these plasma cell membrane vesicles cannot perform the vesicle-substrate fusion to form the SLB by itself. In our works, co-adsorption of synthetic liposomes and plasma cell membrane vesicles facilitates the rupture of cell blebs to form the SLB. This novel strategy is advantageous for incorporating the native membrane species into SLB without involving detergent and reconstitution. The characterization of impact of blebbing conditions on properties of cell blebs, SLB, and membrane species could be the benefits for using bleb bilayer as platform for further biological studies. (Chapter 1) Furthermore, we employed this strategy to create the supported planar stem cell bilayer from adipose derived stem cell. This platform was employed to study the interaction between oncogenic microvesicle and stem cell surface. Uptake of oncogenic microvesicle could lead to the differentiation of stem cell and promote the tumor angiogenesis. However, the binding moieties of microvesicles and the mechanisms of triggering cargo release intra- and extracellularly remain unknown. This platform combined with single particle tracking technique could supply many insights for impact of the microenvironment on the binding of cancer microvesicle and cargo delivery to adipose derived stem cells. (Chapter 2)

REFERENCES

1. Simons, K.; Toomre, D. Lipid rafts and signal transduction. *Nature reviews Molecular cell biology* **2000,** *1* (1), 31-39.
2. Qi, S.; Groves, J. T.; Chakraborty, A. K. Synaptic pattern formation during cellular recognition. *Proceedings of the National Academy of Sciences* **2001,** *98* (12), 6548-6553.
3. Kholodenko, B. N. Cell-signalling dynamics in time and space. *Nature reviews Molecular cell biology* **2006,** *7* (3), 165-176.
4. Gamper, N.; Shapiro, M. S. Regulation of ion transport proteins by membrane phosphoinositides. *Nature Reviews Neuroscience* **2007,** *8* (12), 921-934.
5. Lingwood, D.; Simons, K. Lipid rafts as a membrane-organizing principle. *science* **2010,** *327* (5961), 46-50.
6. Lee, A. G. How lipids affect the activities of integral membrane proteins. *Biochimica et Biophysica Acta (BBA)-Biomembranes* **2004,** *1666* (1), 62-87.
7. Seddon, A. M.; Curnow, P.; Booth, P. J. Membrane proteins, lipids and detergents: not just a soap opera. *Biochimica et Biophysica Acta (BBA)-Biomembranes* **2004,** *1666* (1), 105-117.
8. Helenius, A.; Simons, K. Solubilization of membranes by detergents. *Biochimica et Biophysica Acta (BBA)-Reviews on Biomembranes* **1975,** *415* (1), 29-79.
9. Watts, T. H.; Gaub, H. E.; McConnell, H. M. T-cell-mediated association of peptide antigen and major histocompatibility complex protein detected by energy transfer in an evanescent wave-field. **1986**.
10. Chiantia, S.; Ries, J.; Kahya, N.; Schwille, P. Combined AFM and Two-Focus SFCS Study of Raft-Exhibiting Model Membranes. *ChemPhysChem* **2006,** *7* (11), 2409-2418.
11. Cho, N.-J.; Frank, C. W.; Kasemo, B.; Höök, F. Quartz crystal microbalance with dissipation monitoring of supported lipid bilayers on various substrates. *nature protocols* **2010,** *5* (6), 1096-1106.
12. Terrettaz, S.; Stora, T.; Duschl, C.; Vogel, H. Protein binding to supported lipid membranes: investigation of the cholera toxin-ganglioside interaction by simultaneous impedance spectroscopy and surface plasmon resonance. *Langmuir* **1993,** *9* (5), 1361-1369.
13. Richards, M. J.; Hsia, C. Y.; Singh, R. R.; Haider, H.; Kumpf, J.; Kawate, T.; Daniel, S. Membrane Protein Mobility and Orientation Preserved in Supported Bilayers Created Directly from Cell Plasma Membrane Blebs. *Langmuir* **2016,** *32* (12), 2963-74.
14. Costello, D. A.; Millet, J. K.; Hsia, C.-Y.; Whittaker, G. R.; Daniel, S. Single particle assay of coronavirus membrane fusion with proteinaceous receptor-embedded supported bilayers. *Biomaterials* **2013,** *34* (32), 7895-7904.
15. Costello, D. A.; Hsia, C.-Y.; Millet, J. K.; Porri, T.; Daniel, S. Membrane fusion-competent virus-like proteoliposomes and proteinaceous supported bilayers made directly from cell plasma membranes. *Langmuir* **2013,** *29* (21), 6409-6419.
16. Hopwood, D. A comparison of the crosslinking abilities of glutaraldehyde,

formaldehyde and α-hydroxyadipaldehyde with bovine serum albumin and casein. *Histochemie* **1969,** *17* (2), 151-161.
17. Fraenkel-Conrat, H.; Olcott, H. S. The reaction of formaldehyde with proteins. V. Cross-linking between amino and primary amide or guanidyl groups. *Journal of the American Chemical Society* **1948,** *70* (8), 2673-2684.
18. Sezgin, E.; Kaiser, H.-J.; Baumgart, T.; Schwille, P.; Simons, K.; Levental, I. Elucidating membrane structure and protein behavior using giant plasma membrane vesicles. *Nature protocols* **2012,** *7* (6), 1042-1051.
19. Levental, I.; Lingwood, D.; Grzybek, M.; Coskun, Ü.; Simons, K. Palmitoylation regulates raft affinity for the majority of integral raft proteins. *Proceedings of the National Academy of Sciences* **2010,** *107* (51), 22050-22054.
20. Paulick, M. G.; Bertozzi, C. R. The Glycosylphosphatidylinositol Anchor: A Complex Membrane-Anchoring Structure for Proteins†. *Biochemistry* **2008,** *47* (27), 6991-7000.
21. Nosjean, O.; Briolay, A.; Roux, B. Mammalian GPI proteins: sorting, membrane residence and functions. *Biochimica et Biophysica Acta (BBA)-Reviews on Biomembranes* **1997,** *1331* (2), 153-186.
22. Yeager, C. L.; Ashmun, R. A.; Williams, R. K.; Cardellichio, C. B.; Shapiro, L. H.; Look, A. T.; Holmes, K. V. Human aminopeptidase N is a receptor for human coronavirus 229E. **1992**.
23. Wulfaenger, J.; Niedling, S.; Riemann, D.; Seliger, B. Aminopeptidase N (APN)/CD13-dependent CXCR4 downregulation is associated with diminished cell migration, proliferation and invasion. *Molecular membrane biology* **2008,** *25* (1), 72-82.
24. Ashmun, R. A.; Look, A. T. Metalloprotease activity of CD13/aminopeptidase N on the surface of human myeloid cells. *Blood* **1990,** *75* (2), 462-469.
25. Wurm, F. M. Production of recombinant protein therapeutics in cultivated mammalian cells. *Nature biotechnology* **2004,** *22* (11), 1393-1398.
26. Drexler, I.; Heller, K.; Wahren, B.; Erfle, V.; Sutter, G. Highly attenuated modified vaccinia virus Ankara replicates in baby hamster kidney cells, a potential host for virus propagation, but not in various human transformed and primary cells. *Journal of General Virology* **1998,** *79* (2), 347-352.
27. Zhu, J. Mammalian cell protein expression for biopharmaceutical production. *Biotechnology advances* **2012,** *30* (5), 1158-1170.
28. Vermes, I.; Haanen, C.; Steffens-Nakken, H.; Reutellingsperger, C. A novel assay for apoptosis flow cytometric detection of phosphatidylserine expression on early apoptotic cells using fluorescein labelled annexin V. *Journal of immunological methods* **1995,** *184* (1), 39-51.
29. Vrljic, M.; Nishimura, S. Y.; Moerner, W. Single-molecule tracking. *Lipid Rafts* **2007**, 193-219.
30. Sonnleitner, A.; Schütz, G.; Schmidt, T. Free Brownian motion of individual lipid molecules in biomembranes. *Biophysical Journal* **1999,** *77* (5), 2638-2642.
31. Poudel, K. R.; Jones, J. P.; Brozik, J. A. A guide to tracking single transmembrane proteins in supported lipid bilayers. *Lipid-Protein Interactions: Methods and Protocols* **2013**, 233-252.

32. Ferrari, R.; Manfroi, A.; Young, W. Strongly and weakly self-similar diffusion. *Physica D: Nonlinear Phenomena* **2001,** *154* (1), 111-137.
33. Smith, M. B.; Karatekin, E.; Gohlke, A.; Mizuno, H.; Watanabe, N.; Vavylonis, D. Interactive, computer-assisted tracking of speckle trajectories in fluorescence microscopy: application to actin polymerization and membrane fusion. *Biophysical journal* **2011,** *101* (7), 1794-1804.
34. Sbalzarini, I. F.; Koumoutsakos, P. Feature point tracking and trajectory analysis for video imaging in cell biology. *Journal of structural biology* **2005,** *151* (2), 182-195.
35. Smith, P. R.; Morrison, I. E.; Wilson, K. M.; Fernandez, N.; Cherry, R. J. Anomalous diffusion of major histocompatibility complex class I molecules on HeLa cells determined by single particle tracking. *Biophysical journal* **1999,** *76* (6), 3331-3344.
36. Kusumi, A.; Sako, Y.; Yamamoto, M. Confined lateral diffusion of membrane receptors as studied by single particle tracking (nanovid microscopy). Effects of calcium-induced differentiation in cultured epithelial cells. *Biophysical journal* **1993,** *65* (5), 2021-2040.
37. Hsia, C.-Y.; Chen, L.; Singh, R. R.; DeLisa, M. P.; Daniel, S. A Molecularly Complete Planar Bacterial Outer Membrane Platform. *Scientific Reports* **2016,** *6*.
38. Fuhrmans, M.; Muller, M. Mechanisms of vesicle spreading on surfaces: coarse-grained simulations. *Langmuir* **2013,** *29* (13), 4335-49.
39. Shiratsuchi, A.; Osada, S.; Kanazawa, S.; Nakanishi, Y. Essential role of phosphatidylserine externalization in apoptosing cell phagocytosis by macrophages. *Biochemical and biophysical research communications* **1998,** *246* (2), 549-555.
40. Bortner, C. D.; Cidlowski, J. A. A necessary role for cell shrinkage in apoptosis. *Biochemical pharmacology* **1998,** *56* (12), 1549-1559.
41. Raposo, G.; Stoorvogel, W. Extracellular vesicles: exosomes, microvesicles, and friends. *The Journal of cell biology* **2013,** *200* (4), 373-383.
42. Evdokimovskaya, Y.; Skarga, Y.; Vrublevskaya, V.; Morenkov, O. Secretion of the heat shock proteins HSP70 and HSC70 by baby hamster kidney (BHK-21) cells. *Cell biology international* **2010,** *34* (10), 985-990.
43. Scott, R. E. Plasma membrane vesiculation: a new technique for isolation of plasma membranes. *Science* **1976,** *194* (4266), 743-745.
44. Song, Y. H.; Warncke, C.; Choi, S. J.; Choi, S.; Chiou, A. E.; Ling, L.; Liu, H.-Y.; Daniel, S.; Antonyak, M. A.; Cerione, R. A. Breast cancer-derived extracellular vesicles stimulate myofibroblast differentiation and pro-angiogenic behavior of adipose stem cells. *Matrix Biology* **2016**.
45. Vong, S.; Kalluri, R. The role of stromal myofibroblast and extracellular matrix in tumor angiogenesis. *Genes & cancer* **2011,** *2* (12), 1139-1145.
46. Lee, T. H.; D'Asti, E.; Magnus, N.; Al-Nedawi, K.; Meehan, B.; Rak, J. In *Microvesicles as mediators of intercellular communication in cancer—the emerging science of cellular 'debris'*, Seminars in immunopathology, 2011; Springer, pp 455-467.
47. Soumpasis, D. Theoretical analysis of fluorescence photobleaching recovery experiments. *Biophysical journal* **1983,** *41* (1), 95-97.

48. Hsu, H.-L.; Millet, J. K.; Costello, D. A.; Whittaker, G. R.; Daniel, S. Viral fusion efficacy of specific H3N2 influenza virus reassortant combinations at single-particle level. *Scientific reports* **2016,** *6*.
49. D'Souza-Schorey, C.; Clancy, J. W. Tumor-derived microvesicles: shedding light on novel microenvironment modulators and prospective cancer biomarkers. *Genes & development* **2012,** *26* (12), 1287-1299.
50. Giusti, I.; D'Ascenzo, S.; Millimaggi, D.; Taraboletti, G.; Carta, G.; Franceschini, N.; Pavan, A.; Dolo, V. Cathepsin B mediates the pH-dependent proinvasive activity of tumor-shed microvesicles. *Neoplasia* **2008,** *10* (5), 481-488.
51. Taraboletti, G.; D'Ascenzoy, S.; Giusti, I.; Marchetti, D.; Borsotti, P.; Millimaggi, D.; Giavazzi, R.; Pavan, A.; Dolo, V. Bioavailability of VEGF in tumor-shed vesicles depends on vesicle burst induced by acidic pH. *Neoplasia* **2006,** *8* (2), 96-103.
52. Parolini, I.; Federici, C.; Raggi, C.; Lugini, L.; Palleschi, S.; De Milito, A.; Coscia, C.; Iessi, E.; Logozzi, M.; Molinari, A. Microenvironmental pH is a key factor for exosome traffic in tumor cells. *Journal of Biological Chemistry* **2009,** *284* (49), 34211-34222.
53. Chen, W.-L.; Menzel, M.; Watanabe, T.; Prucker, O.; Rühe, J. r.; Ober, C. K. Reduced lateral confinement and its effect on stability in patterned strong polyelectrolyte brushes. *Langmuir* **2017,** *33* (13), 3296-3303.